nature communications

Article

https://doi.org/10.1038/s41467-025-61807-w

Neural dynamics of spontaneous memory recall and future thinking in the continuous flow of thoughts

Received: 4 October 2024

Accepted: 30 June 2025

Published online: 11 July 2025

Check for updates

Haowen Su[1], Xian Li[2], Savannah Born[3], Christopher J. Honey[2], Janice Chen[2] & Hongmi Lee[1]

Humans constantly recall past experiences and anticipate future events, generating a continuous flow of thoughts. However, the neural mechanisms underlying the natural transitions and trajectories of thoughts during spontaneous memory recall and future thinking remain underexplored. To address this gap, we conducted a functional magnetic resonance imaging study using a think-aloud paradigm, where participants verbalize their uninterrupted stream of thoughts during rest. We found that transitions between thoughts, particularly those involving significant shifts in semantic content, activate the brain's default and control networks. These neural responses to internally generated thought boundaries produce activation patterns resembling those triggered by external event boundaries. Moreover, interactions within and between these networks shape the overall semantic structure of thought trajectories. Specifically, stronger functional connectivity within the medial temporal subsystem of the default network predicts greater variability in thoughts, while stronger connectivity between the control and core default networks is associated with reduced variability. Together, our findings highlight how the default and control networks guide the dynamic transitions and structure of naturally arising memory and future thinking.

The human mind is constantly engaged in recalling the past and predicting the future[1,2]. This creates a continuous stream of thoughts, where semantic memory about the world and oneself, episodic recollections of specific events, and future-oriented simulations are intertwined with information from the current environment[3,4]. Understanding the dynamics of this internally generated thought flow can provide crucial insights into how mental representations are organized in the brain and the neurocognitive processes involved in accessing them. For instance, when people recall memories in a continuous stream, the order and transitions between memories follow underlying semantic and temporal associations; related concepts or events tend to be recalled in succession[5,6]. In addition, transitions between distinct memories evoke characteristic neural responses[7], similar to the neural dynamics observed when continuous external experiences are segmented and organized into discrete event representations[8,9]. However, these findings are primarily derived from studies involving the recall of experimentally induced experiences, such as reading word lists or watching movies[5,7], where task demands control the flow of thoughts. What are the cognitive and neural mechanisms underlying the naturally occurring dynamics of memory and future thinking in real life?

Insights into the processes driving the naturalistic flow of memory and future thinking can be gained through the framework of spontaneous thought. Spontaneous thought refers to thoughts that arise and unfold freely, without being constrained by deliberate cognitive control or attention-capturing salient stimuli[10]. These thoughts mostly

[1]Department of Psychological Sciences, Purdue University, West Lafayette, IN, USA. [2]Department of Psychological and Brain Sciences, Johns Hopkins University, Baltimore, MD, USA. [3]Department of Psychological and Brain Sciences, Washington University in St. Louis, St. Louis, MO, USA.
e-mail: hongmilee@purdue.edu

consist of personally relevant retrospective and prospective memories[4,11], supported by semantic knowledge[3], and often reflect the individual's real-life goals and current concerns[12,13]. In addition, spontaneous thoughts share neural correlates with memory recall and future thinking[1,14–16], particularly involving the default network[17] and the frontoparietal control network[18]. The default network, including the hippocampus, is activated when thoughts are spontaneously generated and maintained[19,20], such as during moments of self-reported mind-wandering[21,22]. The control network is also activated and functionally coupled with the default network during these instances[21,23,24], and is thought to exert top-down control to guide the trajectory of thoughts[10,25].

Despite this extensive research on spontaneous thought, the neurocognitive processes underlying the natural transitions and trajectory of spontaneous memory and future thinking remain underexplored. Common experimental paradigms, such as retrospective reports[26,27] and experience sampling[21,22,26], ask participants to report their thoughts after periods of rest or at intermittent intervals, limiting their ability to track the uninterrupted flow of ongoing thoughts. To address this limitation, recent studies have increasingly used the think-aloud paradigm, where participants verbalize their thoughts in real time during rest[13,28–33], providing a more continuous and detailed report of naturalistic thoughts[30]. These studies have shown that thought trajectories are often clustered, with thoughts staying semantically related until transitioning to new topics, which creates boundaries between thoughts[13,28,29]. Moreover, the variability or stability of thought trajectories has been linked to distinct mental states[33] and individual differences in personality and mental health[29,32]. However, the think-aloud paradigm has rarely been combined with neural recording techniques[30], leaving important questions unanswered about how the brain generates and responds to these transitions and variability in thoughts.

Here, we used the think-aloud paradigm with functional magnetic resonance imaging (fMRI) to investigate the neural correlates of dynamic transitions between thoughts in the flow of spontaneous memory and future thinking. Focusing on the brain's default and control networks, we aimed to address the following questions: (1) What are the major organizing principles guiding transitions from one thought to the next? (2) What are the neural signatures of these thought transitions? and (3) How do brain networks interact to generate variable or stable thought trajectories? We collected think-aloud responses during 10-min resting fMRI scans and segmented them into discrete thought units, each containing a single topic and thought category (e.g., episodic memory, future thinking). By analyzing transition probabilities and semantic similarity between consecutive thoughts, we found that semantic associations primarily guided transitions to related thoughts, although shared neurocognitive processes (i.e., thought categories) also played a role. Strong thought boundaries, characterized by semantic disconnections, activated the default network and adjacent control network areas, resulting in distributed activation patterns similar to those observed at boundaries between external events[7]. Finally, interactions between the default and control network regions shaped the overall semantic structure of thought trajectories. Specifically, stronger functional connectivity within the default network subsystem including the hippocampus predicted greater semantic variability in thoughts, while stronger connectivity between the default and control networks was associated with reduced variability. Together, our findings highlight the central role of the default and control networks in organizing the natural transition dynamics and structure of the unconstrained stream of spontaneous memory and future thinking.

Results

Content and distribution of thoughts

We first examined the content and distribution of various types of thoughts reported during the think-aloud fMRI session. Participants verbally described their stream of spontaneous thoughts for 10 min without interruption. Independent annotators manually segmented these responses into individual thought units based on changes in topic or category of thought (Fig. 1a; see Supplementary Table 1 for examples of segmented thought units). The identified categories were: current state including sensations and feelings (e.g., I feel some breeze), semantic memory about the world or other people (e.g., Baltimore's pretty cool), semantic memory about oneself (e.g., I'm a senior now), episodic memory (e.g., I was walking around earlier with my boyfriend), imagining or planning the future (e.g., I got to go to the grocery store), and other thoughts not fitting into the listed categories. Each thought unit was also assigned a topic label summarizing the content of the thought. Figure 1d visualizes the most frequent words used in topic labels for each thought category, aggregated across all participants.

Participants generated an average of 54.5 thoughts (SD = 19.9, range 19–118), producing an average of 1368.3 words (SD = 376.2, range 368–2268) excluding filler utterances (e.g., Um, what else). Consistent with prior studies[4,34], internally oriented thoughts involving memory and future thinking comprised the majority of spontaneous thoughts (M = 86.8%, SD = 13.6; Fig. 1b). Among these, semantic memory about the world/others was the most frequently reported (M = 28.1%, SD = 12.4), followed by future thinking (M = 24.8%, SD = 19.6), semantic memory about oneself (M = 18.6%, SD = 11.0), and episodic memory recall (M = 15.3%, SD = 11.2). On average, 11.8% of thoughts (SD = 13.3) described current states associated with performing the think-aloud task in the MRI scanner. Only 1.4% of thoughts (SD = 4.1) could not be categorized into one of the five major categories, confirming that our thought categorization scheme effectively captured the content of the think-aloud responses. These differences in relative percentages across categories were statistically significant ($F(5,585) = 55.57$, Greenhouse-Geisser corrected $p < 0.001$, $\eta_p^2 = 0.32$). The five major categories also differed in their average duration per thought ($F(4,344) = 8.05$, Greenhouse-Geisser corrected $p < 0.001$, $\eta_p^2 = 0.09$), with semantic memory about the world/others being the longest. Supplementary Table 2 provides descriptive statistics for each thought category, including mean duration, word count, speech rate, and streak length. For post-hoc paired comparisons of thought categories, see Supplementary Table 3.

The temporal distribution of thought categories over the 10-min think-aloud session showed considerable individual variability (Fig. 1c, upper panel). To examine the group-level temporal distribution, we computed the proportion of participants who reported each thought category in each 1-TR (1.5 s) time window (Fig. 1c, lower panel). The thought categories were generally evenly distributed throughout the session, except that participants disproportionately reported thoughts describing the current state at the beginning of the scan. Specifically, current states comprised 57.6% of the first thoughts reported, suggesting that participants' attention was initially captured by the salient external environment (i.e., being in the MRI scanner) before internally oriented thoughts emerged.

Brain activation for different thought categories

We next examined brain activation associated with different categories of thoughts. First, we conducted a whole-brain analysis to identify the brain areas recruited during spontaneous memory recall and future thinking, in contrast to processing experiences in the immediate environment. For each cortical parcel from the Schaefer 400-parcel atlas[35], we performed paired t-tests comparing the mean activation of each of the four internally oriented thought categories against the current state category. The resulting group-level contrast maps are shown in Fig. 2a, b (Bonferroni corrected, $p < 0.05$). Consistent with prior findings[16,36], both the medial parietal cortex and the lateral parietal cortex within the default network were more strongly activated during the description of internally oriented thoughts compared to the

https://doi.org/10.1038/s41467-025-61807-w

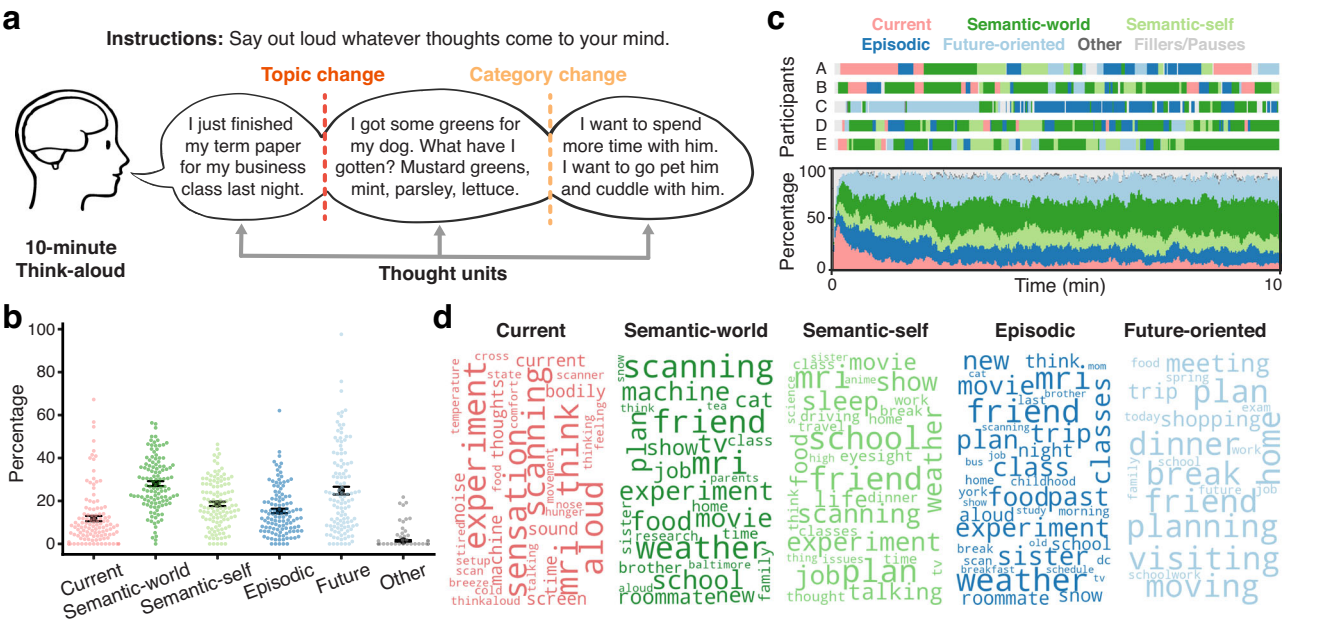

Fig. 1 | Think-aloud verbal responses. a Participants verbally described their spontaneous flow of thoughts for 10 min inside the MRI scanner. Their speeches were transcribed and manually segmented into individual thought units, with each thought unit containing a single topic and corresponding to one of the following categories: current state, semantic memory about the world or other people, semantic memory about oneself, episodic memory, imagining or planning the future, and other uncategorized thoughts. **b** Percentages of different thought categories among all thought units within each participant. Each colored dot represents an individual participant ($N = 118$ for all categories). Black circles indicate the mean across participants within each category. Error bars show the SEM across participants. **c** Temporal distribution of different thought categories within the 10-min think-aloud session. The upper panel shows the distribution of thought categories for five example participants. The lower panel shows the percentages of different thought categories averaged across participants for each time point (1 TR = 1.5-s window). Different colors denote different categories (current state = pink; semantic-world = green; semantic-self = light green; future-oriented = light blue; other = dark gray; fillers/pauses = light gray). **d** Word clouds showing common topics for each major thought category. Topic labels were generated by the annotators who segmented the think-aloud responses. Up to the 50 most frequent words used in topic labels, combined across all participants, are visualized using the WordCloud Python package (version 1.9.3). More frequent words are shown in larger fonts.

current state. This default network activation was more pronounced during episodic recall and future thinking (Fig. 2b) compared to describing generic semantic memory (Fig. 2a), highlighting its involvement in mental time travel and constructive simulation[17,37,38]. In contrast, the temporo-parietal junction, which overlaps with the salience/ventral attention network, was more strongly activated during the current state compared to the other categories. For the list of all suprathreshold parcels from each contrast, see Supplementary Tables 4–7.

Additionally, we examined the activation levels for different thought categories in two subregions of the default network: the posterior medial cortex (PMC) and the hippocampus (Fig. 2c and Supplementary Table 8). Both regions have been frequently implicated in memory retrieval, future thinking, and the generation of spontaneous thoughts[16,36]. Mean activation significantly varied across different thought categories in both PMC ($F(4,224) = 22.72$, $p < 0.001$, $\eta_p^2 = 0.29$) and the hippocampus ($F(4,224) = 5.28$, Greenhouse-Geisser corrected $p = 0.002$, $\eta_p^2 = 0.09$). In PMC, all internally oriented thought categories, except for semantic memory about oneself, showed higher activation compared to the current state ($ts > 2.02$, $ps < 0.048$, Cohen's $ds > 0.37$). Mirroring the whole-brain analysis results, episodic recall and future thinking showed higher activation than semantic memory about oneself or the world ($ts > 4.07$, $ps < 0.001$, Cohen's $ds > 0.65$). Among these, future thinking activated PMC the most, with activation greater than episodic recall ($t(70) = 3.73$, $p < 0.001$, Cohen's $d = 0.61$, 95% CI = [0.04, 0.12]). In the hippocampus, all internally oriented thought categories showed higher activation compared to the current state ($ts > 2.70$, $ps < 0.009$, Cohen's $ds > 0.50$). However, there were no significant differences between the internally oriented thought categories themselves ($ts < 1.91$, $ps > 0.060$, Cohen's $ds < 0.32$). These results remained consistent even after controlling for behavioral measures such as duration, word count, and speech rate for each thought unit (Supplementary Fig. 2).

Transitions between thoughts

An important characteristic of the continuous flow of thoughts is that the mind continually moves from one thought to another[3,28,39], switching between topics and categories (Fig. 1c). What principles underlie the dynamics of these thought transitions? Are there specific mental states that trigger spontaneous memory recall and future thinking? One possibility is that a thought may be evoked by another thought sharing similar neurocognitive processes, such as when memory retrieval is more likely to follow previous memory retrieval than the encoding of new information[40–42]. In this context, a thought is likely to be followed by another from the same category, leading to temporally clustered thought categories. To test this idea, we employed a Markov chain approach that has previously been used to analyze affective transition dynamics in self-generated thoughts[29,43,44]. Specifically, we computed transition probabilities across the six thought categories including the Other category (Fig. 3a). We calculated these probabilities between individual sentences rather than thought units to avoid bias that arises from using category transitions to define thought unit boundaries. Consistent with our prediction, the probability of a thought category transitioning to itself (i.e., the diagonal values of the transition probability matrix) was higher than expected by chance in all thought categories except for the Other category ($ts > 12.78$, $ps < 0.001$, Cohen's $ds > 1.23$; Supplementary Table 9).

Another potential major organizing factor in the chain of thoughts is semantic relations. Models of episodic and semantic memory

https://doi.org/10.1038/s41467-025-61807-w

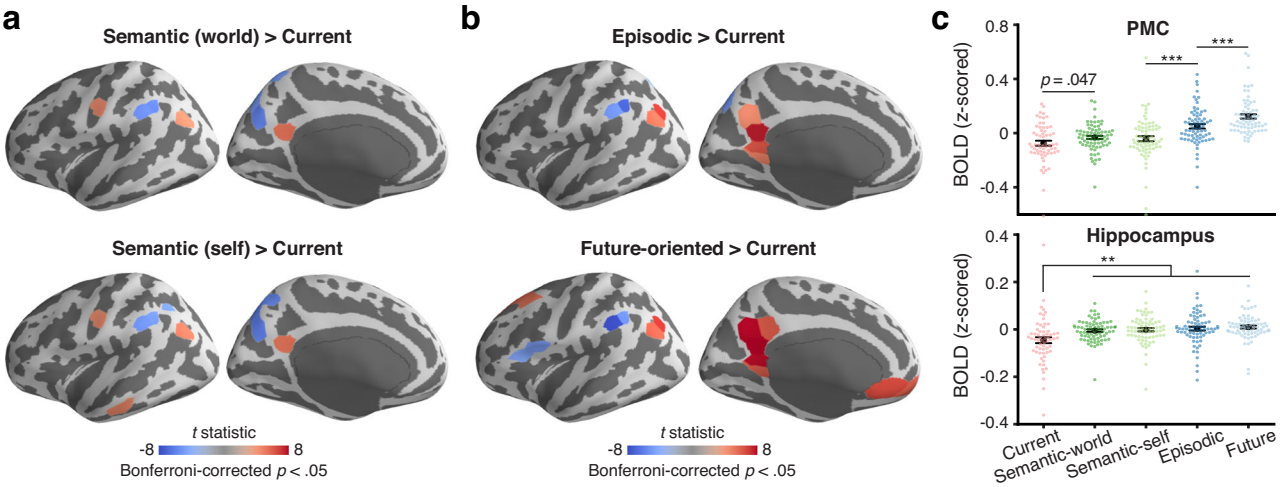

Fig. 2 | Univariate activation during memory recall and future thinking. **a** Whole-brain *t*-statistic maps of cortical parcels showing higher or lower activation while describing semantic memory about the world or other people (top) or about oneself (bottom), compared to describing the current state. **b** Whole-brain *t*-statistic maps of cortical parcels showing higher or lower activation while describing episodic memory (top) or future-oriented thoughts (bottom), compared to describing the current state. In both **a** and **b**, the *t*-statistic maps are displayed on the lateral (left) and medial (right) surfaces of the left hemisphere of the inflated fsaverage6 template brain. Parcels with significantly higher activation compared to the current state are shown in red, while those with significantly lower activation are shown in blue. The statistical significance of each contrast (two-tailed $p < 0.05$) was Bonferroni corrected across the 400 parcels in the Schaefer atlas[35]. Supplementary Tables 4–7 provide the lists of suprathreshold parcels from both hemispheres. Similar activation maps for memory and future thinking were obtained after excluding thought boundary periods from the analysis (Supplementary Fig. 1; see "Neural responses at major thought transitions" in "Results"). **c** Mean blood oxygenation level-dependent (BOLD) signal for each thought category in the posterior medial cortex (PMC; top) and the hippocampus (bottom). Each colored dot represents an individual participant ($N = 62$, 75, 72, 73, and 72 for current, semantic-world, semantic-self, episodic, and future categories, respectively). Black circles indicate the mean across participants within each category. Error bars show the SEM across participants. Statistical significance indicates differences between thought categories based on two-tailed paired *t*-tests. Full statistics for individual comparisons, including exact *p* values, are reported in Supplementary Table 8. $^{**}p < 0.01$, $^{***}p < 0.001$ (uncorrected).

search[5,45,46] and spontaneous thought[13,39] suggest that shared meanings can cue semantically associated thoughts. To test this, we measured semantic similarity between thought units using a natural language processing technique[28,31,33], defining it as the cosine similarity between text embedding vectors representing each thought (Fig. 3b). Supporting the semantic association hypothesis, we found that a thought was semantically more similar to its immediate consecutive thoughts (lags −1 and 1) than to more temporally distant thoughts (lags −15 and 15) across all thought categories ($ts > 9.98$, $ps < 0.001$, Cohen's $ds > 1.22$; Fig. 3c and Supplementary Table 10). The semantic association between consecutive thoughts was particularly stronger for internally oriented thought categories including memory and future thinking, compared to the current state category ($ts > 4.41$, $ps < 0.001$, Cohen's $ds > 0.57$; Supplementary Table 11).

If both shared neurocognitive states (i.e., thought categories) and semantic associations affect transitions between thoughts, which factor has a greater impact? To address this question, we compared thought boundaries involving category changes with those involving topic changes (Fig. 1a and Supplementary Table 1) in terms of their perceived disconnectedness. If semantic associations play a more significant role in the flow of thoughts, then changes in topics (e.g., shifting from episodic recall about a term paper to episodic recall about a dog) will be perceived as stronger boundaries than changes in general thought categories (e.g., shifting from episodic recall about a dog to semantic memory about the dog), and vice versa. To independently measure the perceived strength of boundaries between thoughts, we had a separate group of human coders read the think-aloud transcripts and identify moments when one thought transitioned to another (Fig. 3d). Critically, they were instructed to use their best subjective judgment based on any criteria and were not specifically told to consider changes in thought categories or topics. The measure of boundary strength was boundary agreement scores, computed as the proportion of coders who identified each moment as a thought boundary. The scores ranged from 0 (no coders identified a boundary) to 1 (all coders detected a boundary). Supplementary Fig. 3 presents the full distribution of boundary agreement scores.

The results suggested that semantic associations may play a more crucial role than thought categories in defining thought boundaries. On average, each participant's responses included 21.4 boundaries with category changes alone (SD = 12.2), 13.7 with topic changes alone (SD = 8.5), and 18.4 with both changes (SD = 9.7). Importantly, boundary agreement scores varied across these different types of thought boundaries (Fig. 3e; $F(2,230) = 501.48$, $p < 0.001$, $\eta_p^2 = 0.81$), with higher agreement observed at boundaries involving both topic and category changes ($t(115) = 28.67$, $p < 0.001$, Cohen's $d = 3.00$, 95% CI = [0.39, 0.45]), or topic changes alone ($t(116) = 24.06$, $p < 0.001$, Cohen's $d = 2.27$, 95% CI = [0.32, 0.38]), compared to those involving only category changes. This pattern was mirrored in the semantic similarity between pre- and post-boundary thoughts: semantic similarity was lower at boundaries involving both topic and category changes ($t(115) = 15.29$, $p < 0.001$, Cohen's $d = 1.74$, 95% CI = [0.09, 0.12]) and topic changes alone ($t(116) = 5.57$, $p < 0.001$, Cohen's $d = 0.61$, 95% CI = [0.03, 0.05]), compared to those involving only category changes (Fig. 3f). Furthermore, boundary agreement was negatively correlated with semantic similarity between consecutive thoughts within each participant (mean Spearman's $\rho = -0.33$, SD = 0.16; one-sample *t*-test against zero: $t(116) = -21.62$, $p < 0.001$, Cohen's $d = 2.00$, 95% CI = [−0.36, −0.30]), confirming that changes in semantic content critically influenced thought boundary perception.

Neural responses at major thought transitions

Although internally oriented thoughts generally transition to semantically related ones, shifts to unrelated topics occasionally occur, creating salient boundaries[28,47]. What are the neural signatures of these prominent boundaries between thoughts? While neural responses at event boundaries driven by changes in external stimuli have been

https://doi.org/10.1038/s41467-025-61807-w

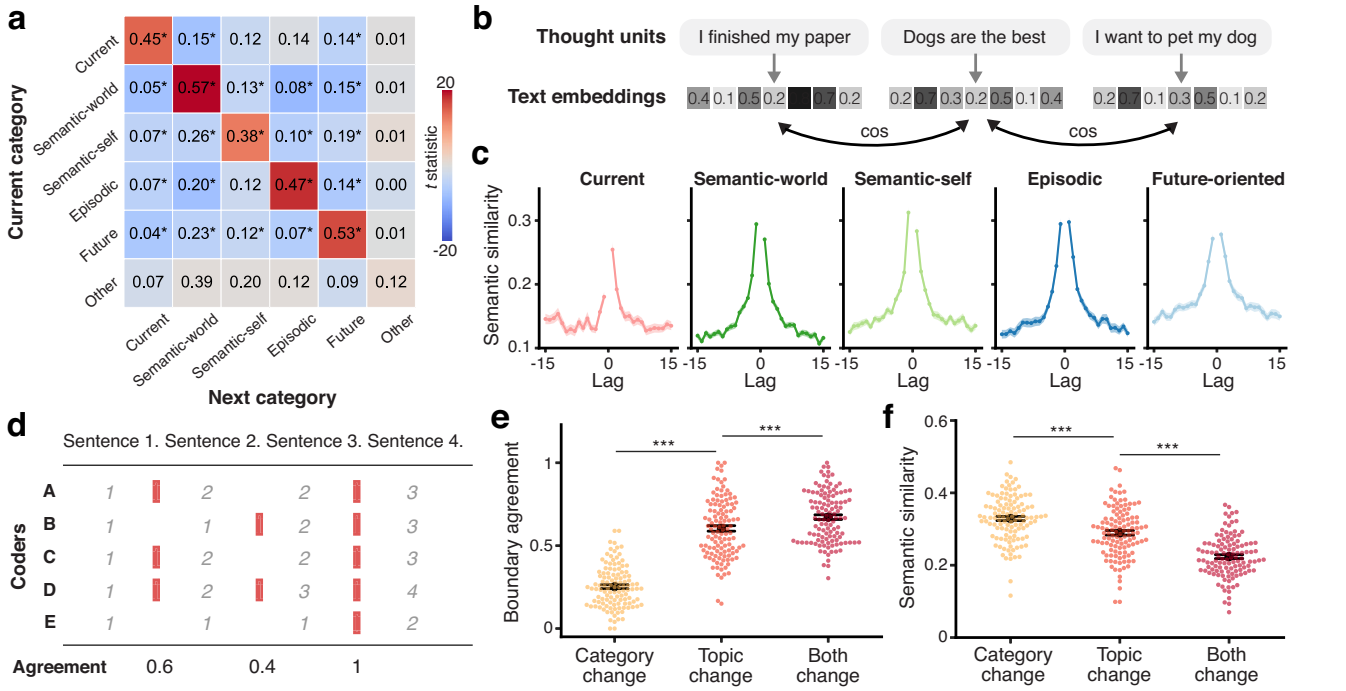

Fig. 3 | Transitions between thoughts. a Sentence-level transition probability between different thought categories. The rows and columns of the matrix represent the current and next categories, respectively. The numbers in the matrix indicate transition probabilities for each category pair, averaged across participants. The colormap of the matrix indicates the *t*-statistics from two-tailed paired *t*-tests against the chance probability (i.e., the overall proportion of the next category among all sentences within each participant). Transitions that occur more frequently than chance are shown in red, while those that occur less frequently than chance are shown in blue. Full statistics for individual cells, including exact *p* values, are reported in Supplementary Table 9. *$p < 0.05$ (Bonferroni corrected). **b** Measuring semantic similarity between thought units. Each thought unit was converted to a text embedding vector using the Sentence Transformers Python module (version 2.2.0). Semantic similarity between thoughts was defined as the cosine similarity between their embedding vectors. **c** Semantic similarity as a function of the temporal distance from a target thought unit in each thought category. Lags are measured in units of thought, with lag = 0 representing the target thought. Negative and positive lags indicate thoughts that occurred before and after the target thought, respectively. Solid lines indicate the mean across participants ($N = 98$, 117, 113, 113, and 112 for current, semantic-world, semantic-self, episodic, and future categories, respectively). Shaded areas indicate the SEM across participants. **d** Measuring thought boundary agreement scores from think-aloud transcripts. Independent coders assigned the same numbers to consecutive sentences/clauses describing a single thought. Thought boundaries (red bars) were detected when the thought identification numbers changed. Boundary agreement scores were defined as the proportion of coders who identified each moment as a thought boundary. **e** Mean boundary agreement scores for different types of thought transitions. **f** Mean semantic similarity between pre- and post-boundary thoughts for different types of thought transitions. In both **e** and **f**, each colored dot represents an individual participant ($N = 117$, 118, and 117 for category change, topic change, and both change conditions, respectively). Black circles indicate the mean across participants within each transition type. Error bars show the SEM across participants. Statistical significance reflects differences between thought transition types, as determined by two-tailed paired *t*-tests. ***$p < 0.001$ (uncorrected).

studied extensively[48–50], internally-driven boundaries between mental contexts have rarely been investigated[7,51]. To characterize the neural responses at boundaries between thoughts, we focused our analysis on the strongest boundaries, defined by a boundary agreement score of 1 (pre- and post-boundary thought semantic similarity: $M = 0.19$, SD = 0.08). These boundaries most commonly involved both thought category and topic changes ($M = 64.5\%$, SD = 22.9), followed by topic change only ($M = 30.4\%$, SD = 21.6) and category change only ($M = 5.1\%$, SD = 9.8). Notably, 81.2% of these strong boundaries involved transitions to one of the four memory/future thinking categories. Supplementary Table 12 provides a breakdown of the percentages for specific thought category pairs that preceded and followed the strong thought boundaries.

We began by identifying the brain areas activated at strong thought boundaries. We performed a whole-brain univariate analysis, contrasting the average activation during boundary periods with that during non-boundary periods (Fig. 4a). A boundary period was defined as a 6-s window following the offset of a pre-boundary thought. A non-boundary period was defined as a 6-s window in the middle of a thought lasting longer than 15 s. Greater activation during boundary periods, compared to non-boundary periods, was observed primarily in the medial frontal and parietal areas of the default network and control network. In contrast, greater activation during non-boundary periods was observed in the lateral frontal areas associated with speech generation and areas around the auditory cortex, reflecting the effect of a temporary pause in speech at thought boundaries. For the list of all suprathreshold parcels, see Supplementary Table 13.

We further examined the activation time course in the PMC and hippocampus ROIs for different types of thought boundaries (Fig. 4b). PMC showed significant activation from 4.5 to 10.5 s following strong thought boundaries, compared to the non-boundary time course aligned to the middle of thoughts ($ts > 4.21$, $ps < 0.001$, Cohen's $ds > 0.66$; Supplementary Table 14). The boundary responses in PMC were also scaled with the strength of thought boundaries. Boundaries involving only topic changes (boundary agreement $M = 0.60$, SD = 0.18) evoked weaker responses compared to the strong boundaries with agreement scores of 1. Boundaries involving only thought category changes (boundary agreement $M = 0.25$, SD = 0.13) resulted in even weaker responses. The hippocampus showed a slightly higher response at 4.5 s following strong boundaries compared to non-boundaries, which did not reach statistical significance ($t(74) = 1.97$, $p = 0.052$, Cohen's $d = 0.37$, 95% CI = [−0.00, 0.08]).

Next, we analyzed the distributed activation patterns at strong thought boundaries. In a prior study[7], we identified a distinctive

https://doi.org/10.1038/s41467-025-61807-w

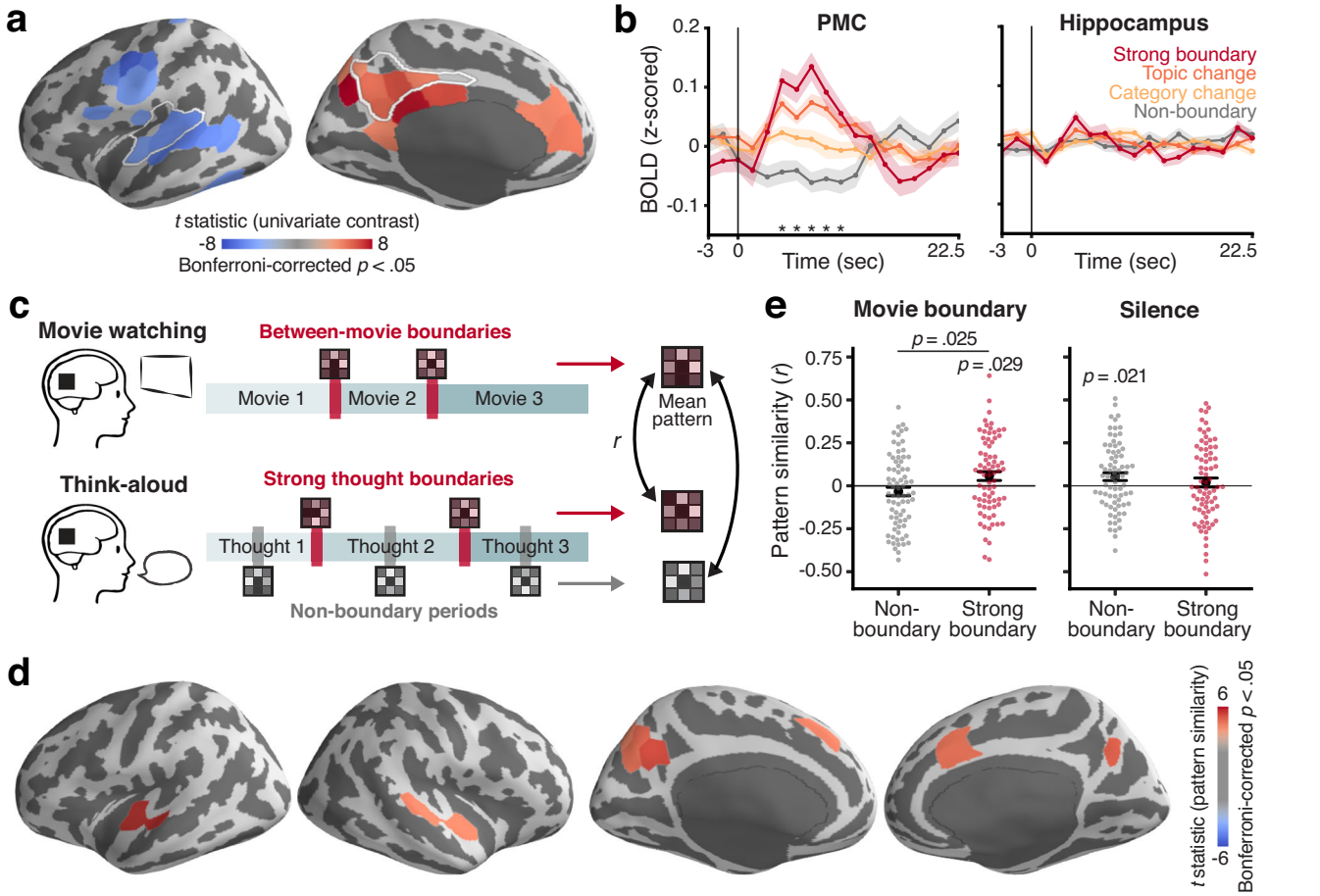

Fig. 4 | Neural responses at thought boundaries. a Whole-brain *t*-statistic map of the univariate contrast between strong boundary (boundary agreement = 1) and non-boundary periods. Parcels with significantly higher activation during strong boundary periods compared to non-boundary periods are shown in red, while those with significantly lower activation are shown in blue. Statistical significance (two-tailed $p < 0.05$) was Bonferroni corrected across all parcels. White outlines indicate the auditory cortex and the posterior medial cortex (PMC), respectively. **b** Mean PMC (left) and hippocampus (right) activation time courses aligned at different types of thought boundaries, with different colors indicating the boundary types (strong boundary = red; topic change = orange; category change = yellow; non-boundary = gray). Time zero for the non-boundary condition represents the middle of thoughts longer than 15 s. For other conditions, time zero represents the offset of the pre-boundary thought. Solid lines indicate the mean across participants ($N = 75$ for all conditions). Shaded areas indicate the SEM across participants. Asterisks above the *x*-axis indicate time points where activation for strong boundaries is significantly higher than non-boundaries, as determined by two-tailed paired *t*-tests with Bonferroni correction ($p < 0.05$). Full statistics for individual time points, including exact *p* values, are reported in Supplementary Table 14. **c** Boundary pattern similarity analysis. For each region, we computed the mean activation pattern of between-movie boundaries from the movie-watching phase of our prior study[7]. This template pattern was correlated with the mean activation patterns of strong thought boundaries (red bars) and non-boundary periods (gray bars) during think-aloud. **d** Whole-brain *t*-statistic map of boundary-specific pattern similarity. Parcels are shown in red if their between-movie boundary patterns were more similar to their strong thought boundary patterns than to the non-boundary patterns. The map is masked to only include areas that showed positive correlations between the between-movie boundary patterns and the strong thought boundary patterns. Statistical significance (two-tailed $p < 0.05$) was Bonferroni corrected across all parcels. **e** Boundary pattern similarity in PMC. The think-aloud strong thought boundary and non-boundary patterns were correlated with the mean activation patterns of between-movie boundary periods (left panel) or silent periods (right panel) from the movie watching phase[7]. Each colored dot represents an individual participant ($N = 75$ for all conditions). Black circles indicate the mean across participants. Error bars show the SEM across participants. Statistical significance relative to zero was assessed using two-tailed one-sample *t*-tests, while differences between conditions were evaluated using two-tailed paired *t*-tests.

activation pattern associated with major mental context transitions within the default network and the adjacent control network, particularly around PMC. Specifically, we observed similar activation patterns at boundaries between different movies while participants watched a series of films. These patterns also reappeared at boundaries between memories of the movies during continuous verbal recall. We predicted that this major mental context transition pattern would generalize to strong thought boundaries during think-aloud sessions.

To test this, we conducted a whole-brain pattern similarity analysis (Fig. 4c). For each cortical parcel, we correlated the mean activation pattern at strong thought boundaries during think-aloud sessions with the mean activation pattern at between-movie boundaries from the movie watching phase of our prior study[7]. We also correlated the mean non-boundary activation pattern during think-aloud with the same between-movie boundary pattern. As predicted, the major mental context transition pattern was observed in parcels within and around PMC. Figure 4d illustrates these parcels, where (1) strong thought boundary patterns were positively correlated with between-movie boundary patterns, and (2) this correlation was greater than the correlation between non-boundary patterns and between-movie boundary patterns. Supplementary Fig. 4 shows separate whole-brain maps of positive pattern similarities between thought boundaries and movie boundaries (Supplementary Fig. 4a) and significant differences between strong thought boundaries and non-boundaries

https://doi.org/10.1038/s41467-025-61807-w

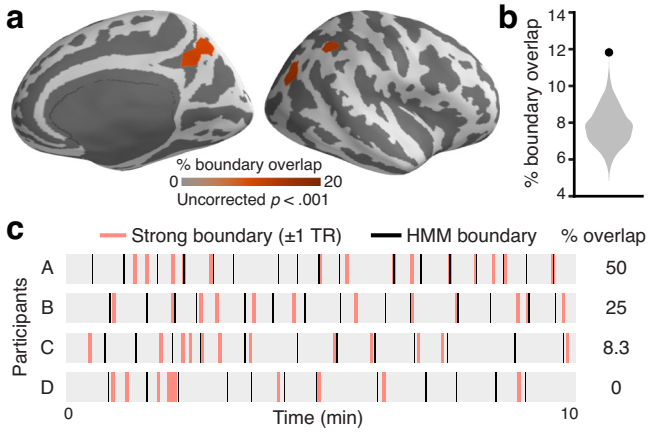

Fig. 5 | Thought segmentation using hidden Markov models (HMM). a Whole-brain map showing the mean percentage of human-identified strong thought boundaries (boundary agreement score = 1) that overlap with parcel-specific HMM-derived boundaries. Parcels with overlap percentages exceeding the null distribution (uncorrected one-tailed randomization $p < 0.001$) are highlighted in red on the right hemisphere of the inflated template brain. A complete list of significant parcels from both hemispheres is available in Supplementary Table 15. **b** Percentage of human-identified strong thought boundaries overlapping with HMM-derived boundaries based on PMC activation patterns. The black dot represents the observed mean across participants ($N = 75$), while the gray distribution represents the null distribution of group means, generated by randomly selecting each participant's strong boundary time points across 1000 iterations. **c** Visualization of human-identified strong thought boundaries (red lines) and HMM-derived boundaries based on PMC activation patterns (black lines) during the 10-min think-aloud sessions of four example participants. An HMM-derived boundary was considered to overlap with a strong thought boundary if it occurred within 1 TR (1.5 s) of the strong boundary. Strong thought boundaries occurring within 2 TRs of excluded TRs (e.g., motion outliers) are not shown.

(Supplementary Fig. 4b). Similar results were observed within the PMC ROI (Fig. 4e, left panel), showing a positive correlation between the strong thought boundary pattern and the between-movie boundary pattern ($t(74) = 2.22$, $p = 0.029$, Cohen's $d = 0.26$, 95% CI = [0.01, 0.11]). This correlation was also greater than the correlation between the non-boundary pattern and the between-movie boundary pattern ($t(74) = 2.29$, $p = 0.025$, Cohen's $d = 0.41$, 95% CI = [0.01, 0.17]).

Is this thought transition pattern simply driven by pauses in speech at boundaries? Strong thought boundaries in the current study and between-movie boundaries in ref. 7 share low-level auditory features, as both involve brief periods of silence. Indeed, parcels around the auditory cortex also showed a positive correlation between strong thought boundary patterns and between-movie boundary patterns (Fig. 4d). To rule out this possibility, we compared the activation patterns at strong thought boundaries with those during periods of silence in the auditory cortex and PMC ROIs. The silence pattern was derived from the movie-watching phase of ref. 7 by averaging silent moments within the movie stimuli. In the auditory cortex (Supplementary Fig. 5), the silence pattern was positively correlated with the strong thought boundary pattern ($t(74) = 4.85$, $p < 0.001$, Cohen's $d = 0.56$, 95% CI = [0.07, 0.18]) but negatively correlated with the non-boundary pattern ($t(74) = -3.17$, $p = 0.002$, Cohen's $d = 0.37$, 95% CI = [−0.10, −0.02]), confirming that its thought boundary pattern was driven by the absence of sound. In contrast, in PMC (Fig. 4e, right panel), the silence pattern was not correlated with the strong thought boundary pattern ($t(74) = 0.73$, $p = 0.465$, Cohen's $d = 0.08$, 95% CI = [−0.03, 0.07]), but was positively correlated with the non-boundary pattern ($t(74) = 2.37$, $p = 0.021$, Cohen's $d = 0.27$, 95% CI = [0.01, 0.10]). Thus, the internally-driven boundary pattern in PMC is unlikely to be driven by pauses in speech.

Shifts in neural representations of thoughts across boundaries

In addition to transient boundary responses, previous studies on stimulus-driven event boundaries have demonstrated shifts in neural representations of extended events across those boundaries, especially in higher-order cortices[52,53]. Do similar shifts occur across thought boundaries during think-aloud? To explore this question, we first examined whether the strong thought boundaries identified by human coders aligned with changes in neural activation patterns detected through a data-driven approach. Specifically, we applied a modified hidden Markov model (HMM) previously used to identify event boundaries in neuroimaging data collected during naturalistic movie viewing and recall[53,54]. The HMM segments continuous brain activity into a predefined number of discrete events, based on the assumption that activation patterns remain stable within each event and shift at event boundaries[53].

We conducted a whole-brain HMM analysis, segmenting the activation time series of each cortical parcel into the same number of segments as the human-identified strong thought boundaries for each participant. Consistent with findings from movie event boundaries[53], the strongest alignment between the human-identified strong thought boundaries and HMM-derived boundaries was observed in parcels within or near the default network, including PMC (Fig. 5a and Supplementary Table 15). Further analysis focusing on PMC also showed significant overlap between the strong thought boundaries and HMM-derived boundaries (% overlap $M = 11.8$, SD = 12.8, one-tailed randomization $p < 0.001$; Fig. 5b, c), suggesting that these strong boundaries corresponded with shifts in neural representations in the region.

We next examined whether changes in neural representations of thoughts across boundaries scaled with perceived boundary strength. We computed PMC pattern similarity between all consecutive thought pairs and correlated these similarity values with boundary agreement scores. To minimize the influence of stereotyped activation patterns at thought boundaries, we excluded 6-second windows following the offset of each thought from the analysis. PMC pattern similarity between consecutive thoughts was negatively correlated with boundary agreement scores (mean Spearman's $\rho = -0.19$, SD = 0.26; $t(74) = -6.37$, $p < 0.001$, Cohen's $d = 0.74$, 95% CI = [−0.25, 0.13]), indicating that greater perceived boundary strength was associated with more pronounced neural shifts in PMC. In both the pattern similarity and HMM analyses, shifts in PMC neural representations were greatest at boundaries involving changes in both thought category and topic, followed by topic-only and category-only changes (see Supplementary Methods).

Thought structure and brain connectivity

So far, we have focused on transitions between immediately neighboring thoughts. However, the dynamics of thought can also be reflected in the overall semantic structure, including the relationships between temporally distant thoughts, such as the recurrence of similar topics over time. Indeed, individuals' thought streams vary in how divergent or focused their content is[10,33]. What are the neural underpinnings of this variability or stability in thoughts? A prominent perspective on spontaneous thought hypothesizes that various large-scale brain networks play distinct roles in shaping the structure of internally oriented thoughts[10]. The medial temporal lobe subsystem of the default network may be responsible for generating variable thoughts, while the core default network subsystem likely constrains thoughts toward personally significant information[55]. The frontoparietal control network (FPCN) may interact with other networks to help sustain goal-relevant thoughts, thereby increasing thought stability[33].

To test this idea, we explored the relationship between functional connectivity within and between large-scale brain networks and the overall semantic structure of think-aloud responses. The semantic structure was quantified using the average clustering coefficient of the semantic network of thoughts, where nodes represented individual

https://doi.org/10.1038/s41467-025-61807-w

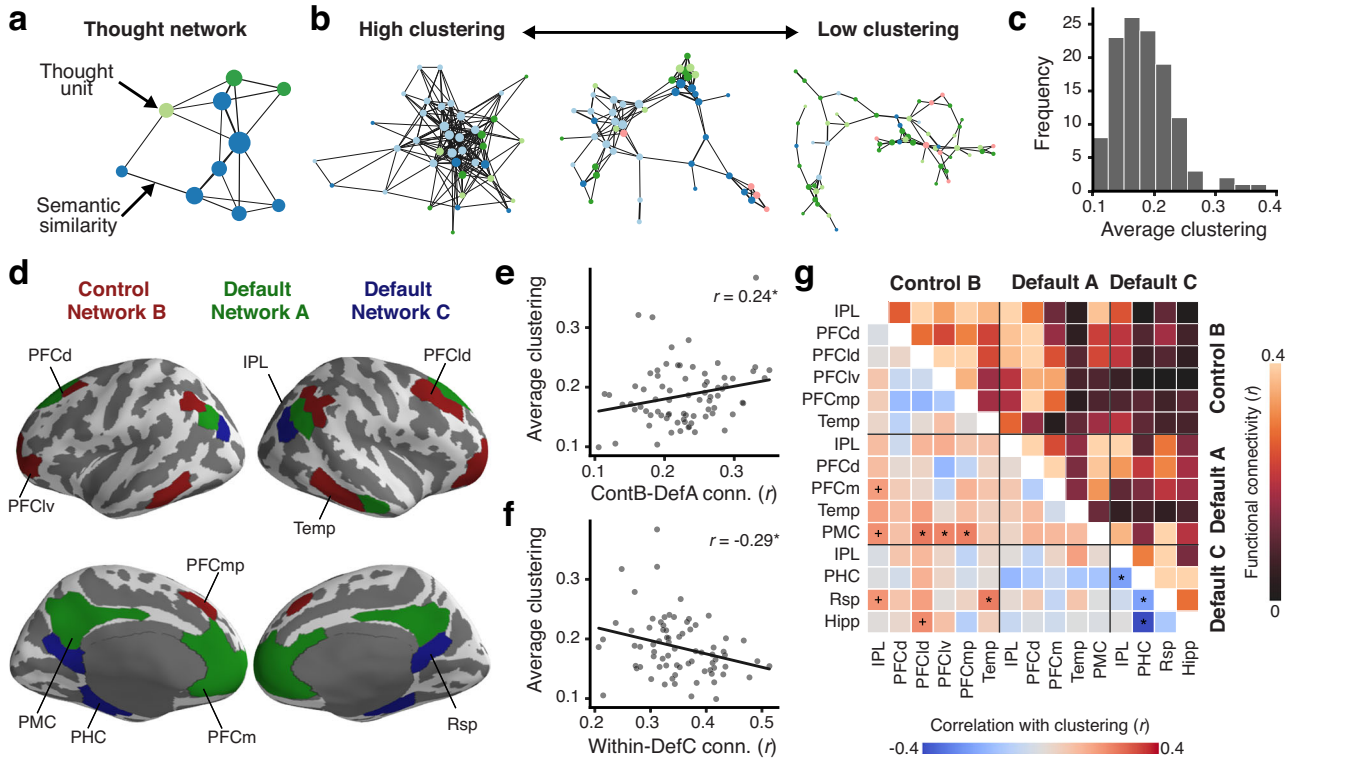

Fig. 6 | Thought network structure and functional connectivity. a A thought network where nodes represent thought units, and edge weights represent semantic similarity between thoughts. **b** Example thought networks with three different levels of clustering (average clustering coefficients = 0.37, 0.27, and 0.19). For visualization, edge weights were thresholded at a cosine similarity of 0.3. In both **a** and **b**, node size and edge thickness are proportional to normalized degree and edge weights, respectively. Different node colors represent different thought categories (pink = current; green = semantic-world; light green = semantic-self; blue = episodic; light blue = future-oriented). **c** Distribution of the average clustering coefficients of thought networks generated from the think-aloud responses of all 118 participants included in the behavioral analyses. Thought network edge weights were thresholded at zero. **d** Subregions of Control Network B (red), Default Network A (green), and Default Network C (blue) as defined in the 17-network version of the 400-parcel Schaefer atlas[35]. The subregions are displayed on the lateral (top) and medial (bottom) surfaces of the inflated fsaverage6 template brain. **e** Pearson correlation between the average clustering coefficients of thought networks and the between-network functional connectivity between Control Network B and Default Network A. **f** Pearson correlation between the average clustering coefficients of thought networks and the within-network functional connectivity in Default Network C. In both **e** and **f**, gray dots represent each of the 75 participants included in fMRI analyses. Solid lines represent the best-fitting regression lines. **g** Mean functional connectivity between the subregions of the three brain networks of interest (upper triangle) and the correlation between the functional connectivity and thought network clustering coefficients (lower triangle). See Supplementary Table 17 for full statistics on subregion pairs that showed a tendency to correlate with thought clustering. Hipp hippocampus, IPL interior parietal lobule, PFCd dorsal prefrontal cortex, PFCld lateral dorsal prefrontal cortex, PFClv lateral ventral prefrontal cortex, PFCm medial prefrontal cortex, PFCmp medial posterior prefrontal cortex, PHC parahippocampal cortex, PMC posterior medial cortex, Rsp retrosplenial cortex, Temp temporal lobe. $^{+}p < 0.1$, $^{*}p < 0.05$ (two-tailed, uncorrected).

thought units and edges represented the semantic similarity between these thoughts (Fig. 6a). Higher clustering coefficients indicated more stable and focused thought structures, while lower clustering coefficients indicated more variable and divergent thought structures (Fig. 6b). Figure 6c shows the distribution of average clustering coefficients across all participants ($M = 0.18$, SD = 0.05). For the functional connectivity analysis, we focused on Control Network B, Default Network A, and Default Network C as defined in the 17-network version of the Schaefer atlas[35], with the hippocampus included in Default Network C (Fig. 6d). These networks correspond, respectively, to a subsystem of the FPCN coupled with the default network[56], the core default network subsystem, and the medial temporal lobe subsystem of the default network, as outlined in ref. 10.

As expected, interaction between the control and default networks was associated with semantic stability in think-aloud responses. Specifically, functional connectivity between Control Network B and Default Network A was positively correlated with thought network clustering coefficients across participants ($r(73) = 0.24$, $p = 0.041$, 95% CI = [0.01, 0.44]; Fig. 6e). Functional connectivity between Control Network B and Default Network C was also numerically positively correlated with clustering coefficients, although this relationship did not reach statistical significance ($r(73) = 0.13$, $p = 0.256$, 95% CI = [−0.10, 0.35]). In contrast, within-network functional connectivity computed across the subregions of Default Network C was negatively correlated with thought network clustering coefficients ($r(73) = -0.29$, $p = 0.013$, 95% CI = [−0.48, −0.06]; Fig. 6f), supporting its role in generating thought variability[10]. There was no significant correlation between clustering coefficients and the connectivity between Default Network A and Default Network C ($r(73) = -0.04$, $p = 0.729$, 95% CI = [−0.27, 0.19]).

Additionally, we performed a post-hoc exploratory analysis to identify specific pairs of subregions whose functional connectivity correlates with the overall semantic structure of thoughts (Fig. 6g, lower triangle; Supplementary Table 16). We found that connectivity between PMC in Default Network A and the lateral dorsal prefrontal, lateral ventral prefrontal, and medial posterior prefrontal cortex subregions in Control Network B was positively correlated with thought network clustering coefficients ($r(73)$s > 0.23, ps < 0.041). Connectivity

between the temporal lobe subregion of Control Network B and the retrosplenial cortex in Default Network C was also positively correlated with clustering coefficients ($r(73) = 0.25$, $p = 0.029$, 95% CI = [0.03, 0.45]). In contrast, within Default Network C, connectivity between the parahippocampal cortex (PHC) and the hippocampus, retrosplenial cortex, and inferior parietal lobule subregions was negatively correlated with thought network clustering coefficients ($r(73)$s < −0.23, ps < 0.044). The strongest of these correlations was between PHC-hippocampus connectivity and clustering coefficients ($r(73) = -0.42$, $p < 0.001$, 95% CI = [−0.59, −0.21]), which survived Bonferroni's correction for multiple comparisons.

Could the correlations between functional connectivity and thought network clustering be driven by boundary-related neural activation? Lower clustering may reflect more frequent or stronger thought boundaries, which could, in turn, increase connectivity among subregions responsive to such boundaries. However, connectivity between Control Network B and Default Network A was positively, rather than negatively, correlated with clustering coefficients (Fig. 6e). Moreover, within Default Network C, clustering coefficients were most negatively correlated with connectivity between the hippocampus and PHC, regions that did not show significant boundary responses, rather than with connectivity involving the retrosplenial cortex, which did (Supplementary Table 13). Thus, boundary-related activation is unlikely to mediate the observed relationships between functional connectivity and thought variability. Functional connectivity and thought variability were also not notably related to the proportions of specific thought categories (see Supplementary Methods).

Discussion

The current study investigated the neural mechanisms underlying the dynamic flow of spontaneous memory recall and future thinking. Using a think-aloud paradigm, where participants continuously verbalized their thoughts during resting fMRI scans, we captured neural responses specifically linked to natural transitions between thoughts and the semantic structure of thought trajectories. Within the flow of thought, primarily consisting of retrospective and prospective memories, transitions predominantly occurred between semantically associated thoughts. Notably, significant shifts in the semantic content of thoughts created boundaries between them, activating core posterior-medial areas of the default and control networks. These boundary responses generated distributed activation patterns comparable to those evoked by boundaries between external events. Furthermore, functional connectivity within and between the default and control networks predicted the overall semantic variability and stability of thought trajectories, highlighting the crucial role of these large-scale networks in shaping the dynamics of spontaneous memory and future thinking.

The think-aloud paradigm enabled us to identify brain regions involved in naturally arising memory and future thinking. Compared to thoughts focused on current feelings and sensations, these internally oriented thoughts—particularly episodic recall and future imagination—activated the default network including the hippocampus, medial frontal cortex, lateral parietal cortex, and PMC. This activation was not systematically influenced by behavioral features such as thought duration, word count, or speech rate (Supplementary Table 2 and Supplementary Fig. 2), suggesting that it reflects deeper cognitive processes rather than superficial features of speech or thought production. Prior studies using more controlled tasks have also implicated a similar set of regions in episodic memory retrieval[15,16], mental simulation[1], and self-referential thinking[19,43], further supporting their role in constructing internal narratives[57]. In addition to the default network, spontaneous thought generation is known to engage broader neural systems, including regions involved in cognitive control[21,23,24]. However, we did not observe notable activation in the control network when compared to the current state category. While the current state category primarily captured thoughts about the immediate environment, the process of consciously accessing and verbalizing them within a continuous stream may demand a similar level of cognitive control as memory and future thinking. This overlap could have diminished the contrast between current state and internally oriented thought categories. Additionally, functional networks beyond the default network show greater inter-individual variability in activation during mind wandering[58], which may have further contributed to the non-significant result.

We found that both shared neurocognitive processes and semantic connections guide the transitions of spontaneous thoughts. Specifically, (1) thoughts tend to transition within the same thought category, and (2) consecutive thoughts show higher semantic similarity than temporally distant ones. This reflects a tendency for thoughts to remain stable for a period before switching to a new one, consistent with prior research describing the locally clustered structure of thought trajectories[3,28,59]. Additionally, topic transitions elicited stronger boundary perceptions and greater cortical activation than thought category transitions, suggesting that semantic connections play a more dominant role in driving spontaneous thought transitions. This finding reinforces the longstanding view that semantic associations provide an organizing framework for internal representations and can serve as retrieval cues[3,5,39,46]. That said, it is worth noting that thought category and semantic content may not be entirely separable. For example, in our study, the current state category predominantly involved semantic content related to the MRI scanning environment (Fig. 1d). A previous study[27] has also reported correlations between temporal dimensions (e.g., past, future) and content-related dimensions (e.g., people, images) in spontaneous thought. Moreover, boundaries involving changes in both thought category and topic were associated with greater semantic shifts than those involving topic changes alone (Fig. 3f), highlighting the influence of thought categories on semantic content. Future research could further investigate how different thought categories and semantic content interact to shape the dynamics and effects of thought transitions.

At strong thought boundaries marked by prominent shifts in thought content, midline default and control network regions are recruited, generating distributed activation patterns similar to those observed at externally-driven event boundaries. Neural responses to stimulus-driven boundaries between external events have been extensively studied in the fields of perception and memory, as they reveal how the brain segments and encodes continuous experiences into discrete events[8,49,50]. However, responses to boundaries created by internal mental context transitions remain largely unexplored[51,60]. In a rare prior study[7], we demonstrated that boundaries between memories of different movies during continuous narrated recall elicit stereotyped activation patterns in PMC and nearby areas, similar to those seen at stimulus-driven movie boundaries during the initial viewing. The current study replicates and expands on these findings, applying them to boundaries between spontaneous internal narratives, which encompass broader semantic topics and exhibit more unconstrained dynamics. Our findings suggest that the boundary responses in the posterior medial areas represent a generalized signal of mental context transitions. This signal likely reflects internal task-switching demands[61,62], which arise at the end of a thought to resolve competition among upcoming thoughts, allowing one to dominate conscious attention. Supporting this idea, the regions with heightened activation at thought boundaries overlapped with posterior-medial areas of the control network (Fig. 4a and Supplementary Table 13). These areas are known to play a key role in top-down cognitive control during task set changes[63,64]. However, this interpretation relies on reverse inference[65], and further research is needed to fully understand the nature of cortical boundary responses in spontaneous thought.

Despite robust cortical responses, we did not observe significant hippocampal activation at major thought boundaries. This was

unexpected given the hippocampus's well-established role in spontaneous thought generation[10,47,66] and mental time travel[36]. Moreover, the hippocampus is consistently activated at externally-driven boundaries between naturalistic events, supporting the successful encoding of these events[49,53,67]. Why, then, does the hippocampus not respond to thought boundaries? One possible explanation is the continuous demand for memory retrieval and thought generation inherent in the think-aloud task. This may lead to sustained hippocampal activation throughout most of the session, masking any responses to thought boundaries, if they exist. Indeed, the hippocampus showed consistently higher activation for memory and future thinking categories, which comprised the majority of thoughts, compared to the current state category where participants simply described their immediate experiences (Fig. 2c and Supplementary Fig. 2). In contrast, during tasks that primarily involve encoding new external events, such as watching movies, the hippocampus may respond specifically to event boundaries by transiently retrieving the just-concluded event[54]. Thus, hippocampal responses differ between externally and internally driven mental context boundaries, despite similar cortical activation patterns.

Beyond transient boundary responses, major thought boundaries were also reflected in shifts in neural patterns associated with pre- and post-boundary thoughts in higher-order cortices, including the default and control networks. Similar pattern shifts have been observed at stimulus-driven event boundaries[52,53]. Importantly, these shifts should be distinguished from the boundary-specific pattern discussed above; rather than reflecting transient responses, they involve changes in the average neural patterns of thoughts or events that remain stable over relatively long timescales. These stable patterns in higher-order cortices, particularly in the default network, are thought to represent abstract internal models of the ongoing situation[53,68]. Our results suggest that such representations may function similarly regardless of whether the information used to build the models is primarily internally generated or externally provided. This supports a recent perspective emphasizing the default network's role in integrating both internal and external sources of information[38].

Our findings demonstrate the role of functional connectivity within and between large-scale brain networks in shaping the semantic structure of spontaneous thought trajectories. This connectivity provides a potential neural basis for individual differences in thought dynamics, ranging from fleeting and freely flowing to more controlled and sustained patterns[69]. Consistent with the dynamic framework of spontaneous thoughts[10], stronger interactions within the medial temporal lobe subsystem of the default network (DN_{MTL}) were linked to greater thought variability, positioning it as a source of variability through associative cueing and pattern completion[39]. In contrast, increased coupling between the control network and the core subsystem of the default network (DN_{core}) was associated with thought stability, confirming the role of the control network in constraining thoughts toward goal-relevant content[55]. These findings also align with creativity research, which suggests that the default network facilitates divergent idea generation, while the control network monitors and evaluates these ideas for goal-relevance[70]. However, connectivity between DN_{MTL} and DN_{core} did not correlate with thought structure, despite the DN_{core}'s proposed role in automatically constraining thoughts toward salient internal information[10]. This may be because automatic constraints can either increase or decrease thought variability depending on its nature[55]. For example, automatic constraints may reduce variability during rumination, when individuals fixate on negative thoughts or emotions. Conversely, they may increase variability by triggering shifts to salient but irrelevant thoughts when attempting to focus on goal-relevant topics.

What are the specific functions of key subregions within these networks that underlie the observed relationships with variable or stable thought structure? Within the DN_{MTL}, the hippocampus represents event memory traces consisting of associations between various contextual details, such as what, where, and when[71]. When a fragment of these details is activated by external input or internal thought, related details are also activated, potentially leading to a cascade of memory retrieval and generating a variable flow of thoughts[39]. This activation of hippocampal memory details can also reinstate their lower-level representations encoded in upstream medial temporal lobe cortices—for example, the spatial layout of a place represented in PHC[72]. Thus, greater coupling between the hippocampus and MTL cortices may reflect the reconstruction of diverse, richly detailed memories. In the DN_{core}, PMC supports the formation and maintenance of abstract internal situation models by integrating external stimuli with memories retrieved by the DN_{MTL}[38], as discussed above. Similarly, the medial prefrontal cortex represents abstract schematic knowledge, especially knowledge related to the self[73]. Together, these regions are thought to support the projection of the self into a mentally constructed situation[74], a process commonly observed during mind-wandering and spontaneous thought. Subregions of the FPCN, particularly the lateral dorsal and lateral ventral (rostrolateral) prefrontal cortices (PFC), likely regulate this process through executive control, sustaining goal-relevant projections while suppressing irrelevant ones[55]. Both regions are implicated in maintaining and implementing task goals and rules, with the lateral dorsal PFC supporting more specific and direct rule implementation than the lateral ventral PFC[10].

Although the think-aloud paradigm has significantly advanced our ability to study the neural dynamics of the continuous flow of thoughts, it still faces important limitations. A major challenge lies in capturing the fully unconstrained and spontaneous nature of real-world thought. Spontaneous thoughts are deeply intertwined with real-life contexts and actions[75], and the fixed setting of verbalizing thoughts in an MRI machine may restrict their natural contents and flow. Moreover, the presence of experimenters and the awareness of being recorded can lead to self-censorship or over-explanation, as indicated by the higher percentage of general semantic descriptions in our data (Fig. 1b, Semantic-world) compared to prior reports[11]. Even without social influences, the very act of consciously accessing and verbalizing thoughts could potentially alter the trajectory of spontaneous thinking[76]. As a result, the cognitive and neural processes engaged during the think-aloud task are likely similar to, but not identical to, those during task-free resting state or real-life mind wandering. Future research may explore how metacognition[77] and the generation of external or internal speech[78] affect the structure and transition dynamics of spontaneous memory and future thinking, as well as the associated neural responses. Another limitation inherent to the think-aloud task is the methodological challenge of parsing and analyzing unconstrained verbal responses. We employed manual segmentation and labeling of thoughts, following the long-standing tradition of using human judgment to annotate natural language data[79]. However, this approach is vulnerable to human error and inconsistencies across annotators, especially when only a single annotator is used per transcript. With recent advances in language models, automated annotation may offer a promising avenue for enhancing both the consistency and scalability of analyzing naturalistic verbal responses in future research[79–81].

In conclusion, our study uncovers the cognitive and neural processes underlying the spontaneous flow of retrospective and prospective memory, bridging the fields of memory and spontaneous thought. Specifically, the default and control networks play a crucial role in thought transitions, and their interactions shape the overall structure of thought trajectories. Understanding these dynamics aids in decoding resting state neural activity[26,27], which has been widely used to explore the neural underpinnings of both clinical conditions and basic cognitive processes. Furthermore, the unfolding of spontaneous thoughts over time reflects the organization of naturalistic thought and predicts individual differences in personality[32,43,59], mental

health[20,29,82], and well-being[83,84]. By investigating the neural mechanisms underlying unconstrained thought dynamics, our findings may inform future research aimed at assessing psychological conditions and developing interventions to support cognitive and emotional health.

Methods

The current study adheres to ethical regulations governing research involving human participants. All experimental procedures were in accordance with protocols approved by the Institutional Review Boards (IRB) of Johns Hopkins Medicine and Homewood.

Participants

We recruited 126 healthy participants from the Johns Hopkins University community (age 18–40 years, mean age 23.7 years). No statistical method was used to predetermine the sample size. Participants' self-reported biological sex indicated that 76 were female and 50 were male. As sex or gender effects were not the primary focus of the current study, these factors were not incorporated into the study design or analysis. All participants were right-handed native English speakers and reported normal hearing as well as normal or corrected-to-normal vision. Informed consent was obtained following procedures approved by the Johns Hopkins Medicine IRB. Participants received monetary compensation for their time ($30 per hour for the fMRI portion and $15 per hour for the behavioral portion).

Of the 126 participants initially recruited, 8 were excluded from both behavioral and fMRI data analyses for the following reasons: poor quality of speech audio recordings (5 participants), scanning interruptions due to technical issues (2 participants), and failure to adhere to instructions (1 participant). An additional 43 participants were excluded from the fMRI data analysis due to: excessive head motion, defined as a mean framewise displacement greater than 0.5 mm (39 participants); anomalies in brain structure (2 participants); technical issues related to visual presentation using the projector (1 participant); and an unidentified artifact in the MRI data (1 participant). Consequently, 118 participants were included in behavioral data analyses (73 females, age 18–39 years, mean age 23.4 years), and 75 participants were included in fMRI data analyses (43 females, age 18–36 years, mean age 23.4 years).

Study procedures

Participants completed a single 10-min think-aloud session in the MRI scanner, during which they verbally described their spontaneous flow of thoughts (Fig. 1a). They were instructed to continuously speak out loud whatever thoughts came to their minds, including but not limited to memories of past events, plans for the future, or any bodily sensations, sights, sounds, or other feelings that captured their attention during the experiment. Participants were instructed to let their thoughts flow freely and not force themselves to stick to a single topic. They were asked not to entertain the experimenter or explain their thoughts by providing background information. Participants were allowed to refrain from verbalizing private thoughts if they did not wish them to be heard. Instead, they were instructed to briefly mention the topic of the thought and state that they did not want to share it (e.g., It reminded me of my parents but I will not talk about it).

Participants began speaking when the word "Begin" appeared in white text on a gray screen. After 2 s, the "Begin" message disappeared, and a white fixation cross was presented at the center, remaining on the screen throughout the task. Participants were instructed to keep their eyes open and look at the fixation cross. However, they were not required to maintain fixation on the cross for the entire task, and their eye movements were not monitored. The visual stimuli were presented on the screen located behind the magnet bore and viewed via an angled mirror, using Psychophysics Toolbox Version 3 (http://psychtoolbox.org). Participants' speech was recorded using an MR-compatible microphone (FOMRI II; Optoacoustics Ltd.) and Audacity software (https://www.audacityteam.org). To reduce speech-induced head motion, participants were instructed to keep their heads still inside the scanner and speak using only their jaw while keeping the rest of their head fixed. The experimenter also demonstrated this technique to participants before each scanning session.

In all but two participants, various tasks unrelated to the current study were performed following the think-aloud task. The remaining two participants performed the think-aloud task at the end of the scanning session, following the unrelated tasks. The unrelated tasks included listening to audio stories, generating word chains, watching screen recording videos, browsing the web, and verbally recalling memories. Different combinations of these tasks were performed in each scanning session, and the results from these tasks will be reported elsewhere.

After the fMRI scanning session, participants received a link to a battery of online questionnaires asking about their personality traits, mental health, and demographic information. They were instructed to complete the questionnaires within 2 days following the fMRI session. Sixty-nine out of the 126 participants completed the questionnaires. Results from the questionnaires will be reported elsewhere.

Behavioral data preprocessing

The audio recording of each participant's think-aloud response was transcribed either manually or automatically using Whisper (Large-v2 model; OpenAI) and subsequently manually corrected. Each transcript was segmented into sentences, and timestamps were identified for the beginning and end of each sentence. Transcribed sentences that ended before the beginning of the scan or began after the end of the scan were excluded from analysis.

The transcripts, formatted with each row corresponding to a single sentence, were further processed by 15 independent human annotators for thought category and topic labeling. Each transcript was handled by a single annotator, with each annotator processing an average of 7.9 transcripts (range: 1–35). Annotators received the transcripts as spreadsheet files and were allowed to work remotely on their personal computers. To promote consistency, all annotators were provided with the same written task instructions. Additionally, two quality-checked transcripts (sub-001 and sub-007) completed by the first annotator were shared as examples for all other annotators to review before beginning the tasks.

First, annotators were instructed to label the category of the thought described in each transcribed sentence by entering a number from 0 to 6 in the Category column of the transcript spreadsheet. The numbers corresponded to the following categories: 0) filler utterances without specific content (e.g., Uh, Um…, What else), 1) current state, action, or sensation during the experiment, 2) memories of past events in specific times or places (e.g., I went hiking yesterday), 3) general knowledge or opinion about oneself (e.g., I like hiking), 4) general knowledge or opinion about the world or other people, 5) imagining or planning the future, and 6) other utterances that cannot be categorized as any of the above categories. No additional instructions were provided, and annotators used their best subjective judgment to categorize each sentence.

Annotators also labeled the topic of the thought described in each sentence. They were instructed to enter a short topic label (ideally 1 to 3 words) in the Topic column of the transcript spreadsheet (e.g., MRI scanning, cold weather, flu shot). For filler utterances, they entered "filler." There was no predefined set of topic labels, and annotators were free to generate any label that best represented the thought. However, to ensure consistency within each transcript, they were instructed to use the same label if the same topic was repeated within a single spreadsheet. In case either the thought category or the topic of the thought changed within a single sentence, annotators were asked to break the sentence into multiple clauses, ensuring that no segment

was coded as having more than one category or topic. During the analysis stage, consecutive sentences or clauses with the same category describing the same topic were combined to form a single thought unit (Fig. 1a). All completed transcripts were manually reviewed for readily identifiable errors, including missing labels and typos. Because each transcript was annotated by a single individual, cross-examination across annotators was not conducted.

Thought category transition probability

To examine how shared neurocognitive states influence thought dynamics, we applied a Markov chain approach, where the probability of a discrete state is predicted based on the previous state. This approach has been previously used to study the structure of transitions between self-generated thoughts with different affective states, such as positive and negative thoughts, and their relationship with personality and mental health[29,43,44]. Here, we extended it to analyze transition probabilities between thought categories likely reflecting general neurocognitive states. Within each participant, these probabilities were computed between individual sentences rather than coarser thought units to avoid bias. Consecutive thought units were biased against belonging to the same category because transitions between thought categories were used to define their boundaries. Six thought categories were analyzed, excluding fillers: current state, semantic-world, semantic-self, episodic, future-oriented, and other (Fig. 3a). For each category, we calculated the proportion of each of the six categories immediately following it. This resulted in a six-by-six transition probability matrix for each participant, where each row represents the current category and each column represents the next category. If a participant's response did not contain a particular category, the transition probabilities from that category (i.e., the row for that category) were considered nonexistent and excluded from the analysis. We then tested whether specific transitions between categories occurred more frequently than expected by chance. For each pair of current and next categories in the transition probability matrix, we performed a two-tailed paired *t*-test, comparing the transition probabilities to the overall proportion of the next category among all sentences generated within each participant.

Semantic similarity between thoughts

To quantify semantic similarity between thoughts, we employed a natural language processing technique that transforms text into embedding vectors. We used a pretrained model (all-mpnet-base-v2) implemented in the Sentence Transformers Python module (version 2.2.0; https://www.sbert.net) to convert the transcribed text of each thought unit into a 768-dimensional vector. Semantic similarity between pairs of thought units was then defined as the cosine similarity between their respective embedding vectors (Fig. 3b).

To examine the effect of temporal proximity on semantic similarity between thoughts, we computed the semantic similarity between each thought unit (i.e., target) and the 15 thoughts preceding and following the target within each participant (Fig. 3c). The semantic similarity as a function of lag from the target was averaged across all target thoughts within each of the five thought categories, excluding Filler and Other. To directly compare thoughts that are near and far from the target, we averaged the semantic similarity at lags 1 and −1 (near) and at lags 15 and −15 (far) within each participant and thought category. We then performed two-tailed paired *t*-tests for each category, using lag (near, far) as a within-participant factor.

To compare the semantic similarity at different types of thought boundaries, we averaged the semantic similarity between consecutive thoughts within each type of boundary: (1) where only the category of thoughts changed, (2) where only the topic of thoughts changed, and (3) where both the category and topic changed. The averaging was done for each participant. We then performed a one-way repeated-measures ANOVA with thought boundary type as a within-participant factor.

Thought boundary agreement

To measure the subjectively perceived strength of boundaries between thoughts without explicitly considering thought categories or topics, we assessed inter-subject agreement on boundary perception using a group of human coders independent from those who annotated thought categories and topics. Inter-subject boundary agreement, widely used in studies of stimulus-driven event boundaries[49,81,85], offers a reasonable proxy for the fMRI participants' own perception of boundaries. Prior studies have shown that individuals tend to converge on which moments constitute boundaries and which do not[86,87], enabling the reliable detection of perceived boundaries even with relatively small samples[88]. Moreover, independently coded boundary agreement has been shown to correlate with neural responses in a separate group of participants[49,85], supporting its validity as a measure of perceived boundary strength.

We recruited 185 coders online from Sona and Prolific to manually segment the think-aloud responses of the 118 fMRI participants. The coders provided informed consent following procedures approved by the Johns Hopkins Homewood IRB. According to the consent form, participation was open to individuals aged 18 to 65 who could understand English. However, no demographic or personal information was collected beyond user identification codes. Coders recruited via Sona received course credit, and those recruited via Prolific were paid $16 per hour.

Each coder was provided with think-aloud transcripts, where each row corresponded to a sentence or clause containing a single thought category and topic. The coders were instructed to use their best subjective judgment to segment each transcript into individual thought units by assigning different numbers to rows representing different thoughts (Fig. 3d). The offset of the last sentence/clause of one thought before a new thought began was identified as the thought boundary. The coders also identified filler utterances that did not correspond to specific thoughts (e.g., uh, um); changes to or from fillers were not considered as thought boundaries. The coders' responses were manually reviewed and deemed problematic if they were (1) incomplete, (2) repeatedly cycling through a small set of thought numbers (e.g., 1,3,2,1,1,2,…), or (3) misclassifying non-filler sentences/clauses as filler utterances. This resulted in the exclusion of data from an additional 19 coders.

Each coder read an average of 3.83 think-aloud transcripts (range: 1–10), and each transcript was segmented by an average of 6 coders (range: 5–8). Boundary agreement was defined as the proportion of coders who identified a given moment as a boundary, serving as a proxy for perceived boundary strength. To compare boundary strength at different types of thought boundaries (i.e., category change only, topic change only, both change) as defined by the manual category and topic coding, we averaged the boundary agreement scores within each participant for each boundary type. We then performed a one-way repeated-measures ANOVA with thought boundary type as a within-participant factor.

MRI data acquisition

MRI scanning was conducted at the F. M. Kirby Research Center for Functional Brain Imaging at Kennedy Krieger Institute on a 3 Tesla Philips Ingenia Elition scanner with a 32-channel head coil. Functional images were acquired using a T2*-weighted multiband accelerated echo-planar imaging (EPI) sequence (TR = 1.5 s; TE = 30 ms; flip angle = 52°; acceleration factor = 4; 60 oblique axial slices; grid size 112 × 112; voxel size 2 × 2 × 2 mm^3). Fieldmap images were also acquired to correct for B0 magnetic field inhomogeneity (60 oblique axial slices; grid size 112 × 112; voxel size 2 × 2 × 2 mm^3). Whole-brain high-resolution anatomical images were acquired using a T1-weighted MPRAGE pulse sequence (150 axial slices; grid size 224 × 224; voxel size 1 × 1 × 1 mm^3).

MRI data preprocessing

MRI data collected during think-aloud sessions were first organized into the Brain Imaging Data Structure (BIDS) format using custom scripts. Preprocessing of high-resolution anatomical images and cortical surface reconstruction were performed using the recon-all pipeline of FreeSurfer[89] (version 7.2.0). Functional images were preprocessed using fMRIprep[90] (version 21.0.2; RRID:SCR_016216) with default settings. Specifically, functional images were corrected for head motion and B0 magnetic inhomogeneity. Functional images were then coregistered to the anatomical image and resampled to the fsaverage6 template surface (for cortical analysis) and the MNI 152 volume space (for subcortical analysis). Additionally, functional images were smoothed (FWHM = 4 mm) in the surface space using FreeSurfer's mri_surf2surf and in the volume space using FSL's SUSAN[91] (Smoothing over Univalue Segment Assimilating Nucleus). To remove high- and low-frequency drift and noise related to motion, physiological responses, and scanner artifacts, nuisance regressors including linear and quadratic trends, six head motion parameters (translation and rotation in the x, y, and z dimensions), and the average time courses of the whole-brain mask, cerebrospinal fluid, and white matter were then projected out from the smoothed data. To preserve signals associated with the think-aloud task, additional bandpass filtering was not applied. The resulting time series were z-scored within each vertex or voxel across all volumes within the scanning run. Within each scanning run, the first 10 volumes were discarded. Motion outlier volumes (framewise displacement ≥1 mm), along with the two volumes immediately preceding and following each outlier, were also excluded from the analysis.

Cortical parcellation and region of interest (ROI) definition

For whole-brain activation and pattern similarity analyses, we used a cortical parcellation atlas based on functional connectivity patterns identified through fMRI[35]. The atlas divides the cortical surface into 400 parcels, with 200 parcels in each hemisphere, which are grouped into 17 functional networks identified in a previous study[92].

For region-of-interest analyses, we defined the bilateral posterior-medial cortex (PMC) and the bilateral auditory cortex (Fig. 4a) by combining parcels from the 400-parcel atlas that correspond to the regions. The PMC ROI included parcels from the posterior cingulate cortex and precuneus within Default Network A. The auditory cortex ROI consisted of parcels around the primary and secondary auditory cortices within Somatomotor Network B (see Supplementary Table 17 for the list of parcels included in the ROIs). The bilateral hippocampus mask was obtained from the subcortical atlas (Aseg) provided by FreeSurfer, using the MNI volume space as reference.

For functional connectivity analysis, we extracted individual subregions from three a priori functional networks of interest out of the 17 networks in the atlas: Control Network B, Default Network A, and Default Network C (Fig. 6d). Parcels corresponding to each subregion defined by the atlas were combined to form a single region. Control Network B consisted of subregions in the interior parietal lobule (IPL), dorsal prefrontal cortex (PFCd), lateral dorsal prefrontal cortex (PFCld), lateral ventral prefrontal cortex (PFClv), medial posterior prefrontal cortex (PFCmp), and temporal lobe. Default Network A consisted of subregions in the IPL, PFCd, medial prefrontal cortex (PFCm), temporal lobe, and PMC. Default Network C consisted subregions in the IPL, parahippocampal cortex (PHC), and retrosplenial cortex (Rsp). Additionally, we included the hippocampus as a subregion of Default Network C.

Univariate activation for different thought categories

We performed whole-brain univariate activation analysis to identify regions recruited during spontaneous memory recall and future thinking. For each participant, we computed the mean activation for each thought category within each cortical parcel from the 400-parcel atlas. This was done by first averaging the preprocessed blood oxygenation level-dependent (BOLD) signal across all vertices within a parcel and across TRs within each thought unit. We then averaged these mean signals across thought units corresponding to each thought category. Next, for each parcel, we performed group-level contrasts between the current state category and each of the other thought categories of interest (i.e., semantic-world, semantic-self, episodic, and future-oriented) using two-tailed paired t-tests. The current state category served as an active baseline because it involved speech, like the other categories, but reflected processing of the immediate environment without engaging memory recall or future thinking. These contrasts resulted in whole-brain t-statistic and p-statistic maps for each of the four comparisons. We applied Bonferroni's correction to each contrast map to account for multiple comparisons across all 400 parcels.

We also repeated this whole-brain analysis after excluding TRs corresponding to thought boundary periods to account for neural responses at thought transitions (Supplementary Fig. 1; see "Neural responses at major thought transitions" in "Results"). A boundary period was defined as a 6-s window beginning at the offset of the thought immediately preceding a strong thought boundary (boundary agreement score = 1), shifted forward by 4.5 s to account for the hemodynamic response delay.

We additionally compared univariate activation across thought categories within the PMC and hippocampus ROIs. For each participant and ROI, we computed the mean activation for each thought category by averaging the preprocessed BOLD signal across vertices/voxels and across TRs within each thought unit, and then averaging across all thought units corresponding to each category. For each ROI, we performed a one-way repeated-measures ANOVA with the thought category as a within-subject factor to test for statistically significant differences in activation across thought categories.

Finally, we examined PMC and hippocampus ROI activation across different thought categories while controlling for potential behavioral confounds, including thought-specific duration, word count, and speech rate (duration divided by word count). For each behavioral measure, we regressed it out from the thought-wise mean activation level of each ROI within each participant. The resulting residual activation values were then used to compare group mean activation across thought categories, following the same procedures described above. For all whole-brain and ROI analyses, the time windows corresponding to individual thought units were shifted forward by 4.5 s to account for the hemodynamic response delay.

Univariate activation at thought boundaries

We first performed a whole-brain analysis (Fig. 4a) to identify brain regions activated at strong thought boundaries, defined as those with boundary agreement scores of 1. For each cortical parcel in each participant, we computed the mean activation during strong thought boundary periods and non-boundary periods. A strong boundary period was defined as a 6-second window starting at the offset of the thought that immediately preceded a strong boundary. A non-boundary period was defined as the 6-s window in the middle of thoughts lasting longer than 15 s. To account for the hemodynamic response delay, both boundary and non-boundary time windows were shifted forward by 4.5 s. This selection of time bins enabled us to capture the peak boundary response periods (Fig. 4b) while minimizing potential overlap between strong boundary and non-boundary periods. In our data, these periods did not overlap except for a single TR in one participant, which was excluded from the analysis. Preprocessed BOLD signals were first averaged across all TRs within the boundary/non-boundary periods and then across vertices within each parcel. Next, for each parcel, we performed a group-level contrast between the strong boundary periods and non-boundary periods using two-tailed paired t-tests. The resulting whole-brain t-statistic

map was corrected for multiple comparisons across all 400 parcels using Bonferroni's method.

We also examined activation time courses evoked by different types of thought boundaries in the PMC and hippocampus ROIs. For each participant and ROI, we averaged TR-by-TR activation across all vertices/voxels within the ROI. From this activation time series, we extracted 27-s (18 TRs) time courses locked to thought boundaries (i.e., from 2 TRs before to 15 TRs after the thought offset TR). The time courses were then averaged across boundaries within each boundary type: (1) strong thought boundaries with boundary agreement scores of 1, (2) boundaries where only the topic of thoughts changed, and (3) boundaries where only the category of thoughts changed. For the non-boundary control condition, we additionally extracted and averaged time courses locked to the middle of thoughts lasting longer than 15 s (i.e., from 2 TRs before to 15 TRs after the middle TR). Two-tailed paired *t*-test were performed to compare activation levels between boundary and non-boundary conditions at each time point of the time courses. Bonferroni's correction was applied to correct for multiple comparisons across the 18 time points.

Distributed activation pattern at thought boundaries

We conducted a whole-brain pattern similarity analysis to test if the major mental context transition pattern observed in our prior study[7] generalized to strong thought boundaries during the think-aloud task (Fig. 4c). We first extracted strong thought boundary and non-boundary patterns for each cortical parcel in each participant's brain. A strong thought boundary pattern was generated by averaging activation patterns across all TRs within 6-s windows starting from the offset of thoughts immediately preceding strong boundaries with an agreement score of 1. A non-boundary pattern was generated by averaging activation patterns across all TRs within the middle 6 s of thoughts lasting longer than 15 s. To account for the hemodynamic response delay, both boundary and non-boundary time windows were shifted forward by 4.5 s. As before, the strong boundary and non-boundary periods did not overlap, except for a single TR in one participant, which was excluded from the analysis.

We next computed Pearson correlations between the think-aloud boundary/non-boundary patterns and the between-movie boundary pattern obtained from the movie watching phase data of our prior fMRI study[7]. In that study, participants watched a series of ten short (2–8 min long) audiovisual movie stimuli, separated by 6-s title scenes. Participants subsequently verbally recalled the movies in any order they wanted. To preserve the between-movie boundary pattern reported in the original study as closely as possible, the dataset was preprocessed following the pipeline described in ref. 7. This pipeline included motion correction, B0 unwarping, coregistration to the fsaverage6 cortical surface, spatial smoothing (FWHM = 4 mm), high-pass filtering (cutoff = 140 s), and *z*-scoring within each functional run. We then followed the procedures described in ref. 7 to generate the between-movie boundary pattern for each participant. Activation patterns were first averaged across time points within the 15-s boundary period following the offset of each movie, shifted forward by 4.5 s. These patterns were then averaged across all movie stimuli. The resulting activation patterns showed consistently positive correlations across the fifteen participants analyzed (mean intersubject Pearson $r = 0.404$, SD = 0.096). Finally, the patterns were averaged across participants to generate a single, robust template pattern.

To test whether the strong boundary patterns were overall positively correlated with the between-movie boundary patterns, we performed group-level two-tailed one-sample *t*-tests against zero on the correlation coefficients for each cortical parcel. Additionally, group-level two-tailed paired *t*-tests were performed to directly compare the similarity of the between-movie boundary patterns to the strong thought boundary patterns versus the non-boundary patterns. Bonferroni's correction was applied to each resulting whole-brain statistical parametric map to correct for multiple comparisons across parcels. Finally, to identify parcels showing significant effects in both tests after correction, we masked the areas with higher similarity to the strong boundary pattern compared to the non-boundary pattern with the areas that showed overall positive similarity to the strong boundary pattern. We also performed the same boundary pattern similarity analysis within the PMC and auditory cortex ROIs, as was done for individual parcels in the whole-brain analysis.

Finally, we tested whether the strong thought boundary patterns in the PMC and auditory ROIs were influenced by temporary silence due to pauses in speech at the boundaries. To do this, we compared the think-aloud boundary/non-boundary patterns with the activation pattern associated with silence, measured during the movie watching phase of ref. 7. Silent periods were defined as moments in the movies when the audio amplitude, convolved with a hemodynamic response function, fell to the mean amplitude observed during the title scenes between movies with no sound. To prevent potential carryover effects from the between-movie boundaries, we excluded time points within the first 45 s of each movie from the silent periods. Activation patterns were averaged across all time points within the silent periods for each participant and then across participants. We performed group-level two-tailed one-sample *t*-tests against zero to test the overall positivity of correlations between the silence template pattern and the think-aloud boundary/non-boundary patterns. Additionally, we performed two-tailed paired *t*-tests to compare the similarity of the silence template pattern to the strong thought boundary versus the non-boundary patterns.

Hidden Markov model analysis

To segment thoughts in a data-driven manner based on changes in neural activation patterns, we applied a modified hidden Markov model (HMM) that has been previously used to detect event boundaries in neuroimaging data collected during naturalistic movie watching and recall[53,54]. The HMM segments continuous brain activity time series into a predefined number of discrete events, or hidden states, based on the assumption that activation patterns remain relatively stable within each event and shift to a new stable pattern at event boundaries, reflecting a transition from one event to the next[53].

We first conducted a whole-brain analysis to identify brain regions where HMM-derived thought boundaries aligned with human-identified strong thought boundaries (boundary agreement score = 1). For each cortical parcel in each participant's brain, we fit the HMM to the time course of its activation patterns using the event segmentation module in the Brain Imaging Analysis Kit Python package (version 0.12; https://brainiak.org). The number of events was set to match the number of segments defined by the participant's strong boundaries, excluding any segments that fell entirely within TRs omitted from analysis (e.g., motion outlier periods). We then calculated the percentage of strong boundaries that overlapped with the HMM-derived boundaries. An HMM-derived boundary was considered overlapping if it occurred within a 3-TR window centered on the strong boundary (including the strong boundary TR itself and the TRs immediately before and after it), shifted forward by 4.5 s to account for the hemodynamic response delay. To avoid confounds from excluded TRs, strong boundaries occurring within 2 TRs of excluded TRs were not included in the overlap calculation. Finally, we averaged the percent overlap values across participants to obtain the group mean for each parcel. We also applied the HMM analysis to the PMC ROI, using the same procedures as for individual parcels in the whole-brain analysis.

To assess the statistical significance of the percentage overlap between HMM-derived and human-identified strong thought boundaries, we conducted a randomization test for each region, comparing the actual group mean to a null distribution of group

means. To generate the null distribution, we randomly selected 3-TR boundary windows within each participant, ensuring that these windows did not overlap with each other and were at least 2 TRs away from excluded TRs. The number of random boundary windows matched the number of strong boundaries included in the analysis for each participant. Next, we computed the group mean percentage overlap between HMM-derived boundaries and these randomly selected boundaries. This process was repeated 1000 times to generate the null distribution. The one-tailed p value was defined as the proportion of all percentage overlap values, including the observed group mean, that were greater than or equal to that observed value. The lowest possible p value was 0.000999 (1/1001), which occurred when the actual group mean exceeded all values in the null distribution.

Pattern similarity between consecutive thoughts

To examine the relationship between thought boundary strength and neural similarity between pre- and post-boundary thoughts, we analyzed thought-specific distributed activation patterns in the PMC. Within each participant, we first computed the mean PMC activation pattern for each thought by averaging activation across TRs corresponding to that thought. We then calculated Pearson correlations between the activation patterns of consecutive thoughts. To minimize the effects of boundary-related responses, we excluded 6-s windows following each thought offset. Both the time windows corresponding to individual thought units and the excluded boundary windows were shifted forward by 4.5 s to account for the hemodynamic response delay. If a thought unit fell entirely within an excluded window, its pattern similarity with neighboring thoughts could not be computed. As a result, an average of 38.1% of consecutive thought pairs remained for analysis (SD = 19.1). We then computed a correlation between the remaining pattern similarity values and boundary agreement scores for the corresponding boundaries. Spearman correlation was used because the boundary agreement scores were not normally distributed (Supplementary Fig. 3). The resulting subject-specific correlation coefficients were tested against zero at the group level using a two-tailed one-sample t-test.

Thought network structure

To quantify the overall structure of think-aloud responses, we transformed each participant's response into a semantic network (Fig. 6a) following the procedures developed in our prior study[93]. In this network, the nodes represented individual thought units, and the edges between nodes represented the semantic similarity between thoughts. Semantic similarity between all possible pairs of thoughts was measured using the procedures described above in the "Semantic similarity between thoughts" section. Specifically, each thought unit was converted into a 768-dimensional text embedding vector, and the cosine similarity between these vectors was computed. The resulting network was undirected, and edges with weights below zero were removed. To measure the global structure of the thought network, we calculated the average clustering coefficient across all nodes (Fig. 6b). The clustering coefficient for each node was defined as the geometric average of the subgraph edge weights, using the implementation provided by the NetworkX Python package (version 3.1; https://networkx.org).

Functional connectivity analysis

To examine how interactions between brain regions influence the overall structure of thought networks, we computed functional connectivity within and between brain networks involved in spontaneous thought generation[10,23,55]. Specifically, we focused on Control Network B, Default Network A, and Default Network C as defined in the 17-network version of the 400-parcel cortical atlas[35]. Among the three subnetworks of the control network (A, B, and C), Control Network B specifically corresponds to the frontoparietal control network subsystem ($FPCN_A$) previously identified as positively coupled with the default network[56]. Default Network A and Default Network C correspond to the core default network subsystem and the medial temporal lobe subsystem of the default network, respectively, as discussed in prior studies[10,55].

Functional connectivity was computed from the entire think-aloud session for each participant. First, we extracted the mean activation time course of each network subregion by averaging across all vertices/voxels within each region and hemisphere. For bilateral subregions, time courses were also averaged across hemispheres (see Fig. 6d and the "Cortical parcellation and region of interest definition" section above for the list of subregions). Next, we computed pairwise Pearson correlations between the activation time courses of individual subregions. Within-network functional connectivity was then defined as the average of correlations between different subregions within the same network. Between-network functional connectivity was defined as the average of correlations between all possible pairs of subregions across two different networks.

Finally, we computed Pearson correlations between the participant-wise average thought network clustering coefficients and the within/between-network functional connectivity values. We specifically examined four connectivity measures hypothesized to be associated with thought structure[10,55]: three between-network connectivity values (Control B–Default A, Control B–Default C, and Default A–Default C) expected to be positively correlated with clustering, and one within-network connectivity for Default Network C, expected to be negatively correlated with clustering. Because we tested a small number of theory-driven, a priori hypotheses with specific directional predictions, we did not apply multiple comparisons correction across these network-level connectivity measures.

As a post hoc exploration, we also computed correlations between the thought network clustering coefficients and the functional connectivity between all individual subregions in the three brain networks. Bonferroni's correction was applied to correct for multiple comparisons across all possible pairs of subregions. Additionally, for exploratory purposes, we conducted supplementary analyses examining (1) the relationship between thought network clustering and functional connectivity involving Control Network A, a subsystem of FPCN not strongly coupled with the default network[56], and (2) the relationship between functional connectivity and the proportions of different thought categories (see Supplementary Methods).

Statistical tests

Statistical tests were performed using the Scipy (version 1.12.0; https://scipy.org) and Pingouin (version 0.5.1; https://pingouin-stats.org) Python packages, along with custom scripts. Details of the statistical tests used in each analysis are provided in the corresponding subsection of the "Methods" section. All statistical tests were two-tailed, except for the one-tailed nonparametric randomization tests used in the HMM analysis. For parametric tests comparing means across multiple conditions, Mauchly's test was used to assess sphericity. If the assumption of sphericity was violated, the Greenhouse-Geisser corrected p value was reported in place of the uncorrected p value. Only participants with complete data for all relevant conditions were included in comparisons. Participants with missing data in any condition (e.g., those who did not generate thoughts in the current state category when comparing current state and episodic recall) were excluded from the relevant comparisons.

Reporting summary

Further information on research design is available in the Nature Portfolio Reporting Summary linked to this article.

Data availability

The raw fMRI and behavioral data from the think-aloud sessions have been deposited on OpenNeuro.org under accession number ds006067 [https://doi.org/10.18112/openneuro.ds006067.v1.0.0][94]. Additional data needed to reproduce the results (e.g., independent thought boundary segmentations, text embeddings) are available on Zenodo [https://doi.org/10.5281/zenodo.15665444][95]. The previously published fMRI dataset used to generate the between-movie boundary pattern is also available on OpenNeuro.org under accession number ds004042 [https://doi.org/10.18112/openneuro.ds004042.v1.0.1][96,97].

Code availability

All analyses in this study were conducted using publicly available MRI data processing software (e.g., FSL, FreeSurfer) and Python packages. The analysis scripts used to generate the display items in this paper are available on Zenodo [https://doi.org/10.5281/zenodo.15665444][95]. Other analysis scripts are available upon request to the corresponding author (H.L.).

References

1. Schacter, D. L., Addis, D. R. & Buckner, R. L. Remembering the past to imagine the future: the prospective brain. *Nat. Rev. Neurosci.* **8**, 657–661 (2007).
2. Bar, M. The proactive brain: memory for predictions. *Philos. Trans. R. Soc. B Biol. Sci.* **364**, 1235–1243 (2009).
3. Mildner, J. N. & Tamir, D. I. Spontaneous thought as an unconstrained memory process. *Trends Neurosci.* **42**, 763–777 (2019).
4. Smallwood, J. & Schooler, J. W. The science of mind wandering: empirically navigating the stream of consciousness. *Annu. Rev. Psychol.* **66**, 487–518 (2015).
5. Polyn, S. M., Norman, K. A. & Kahana, M. J. A context maintenance and retrieval model of organizational processes in free recall. *Psychol. Rev.* **116**, 129–156 (2009).
6. Diamond, N. B. & Levine, B. Linking detail to temporal structure in naturalistic-event recall. *Psychol. Sci.* **31**, 1557–1572 (2020).
7. Lee, H. & Chen, J. A generalized cortical activity pattern at internally generated mental context boundaries during unguided narrative recall. *eLife* **11**, e73693 (2022).
8. Zacks, J. M. et al. Human brain activity time-locked to perceptual event boundaries. *Nat. Neurosci.* **4**, 651–655 (2001).
9. Reagh, Z. M., Delarazan, A. I., Garber, A. & Ranganath, C. Aging alters neural activity at event boundaries in the hippocampus and posterior medial network. *Nat. Commun.* **11**, 3980 (2020).
10. Christoff, K., Irving, Z. C., Fox, K. C. R., Spreng, R. N. & Andrews-Hanna, J. R. Mind-wandering as spontaneous thought: a dynamic framework. *Nat. Rev. Neurosci.* **17**, 718–731 (2016).
11. Baird, B., Smallwood, J. & Schooler, J. W. Back to the future: autobiographical planning and the functionality of mind-wandering. *Conscious. Cogn.* **20**, 1604–1611 (2011).
12. Klinger, E. Goal commitments and the content of thoughts and dreams: basic principles. *Front. Psychol.* **4**, 415 (2013).
13. Mildner, J. N. & Tamir, D. I. Why do we think? the dynamics of spontaneous thought reveal its functions. *PNAS Nexus* **3**, pgae230 (2024).
14. Kim, H. An integrative model of network activity during episodic memory retrieval and a meta-analysis of fMRI studies on source memory retrieval. *Brain Res.* **1747**, 147049 (2020).
15. Rugg, M. D. & Vilberg, K. L. Brain networks underlying episodic memory retrieval. *Curr. Opin. Neurobiol.* **23**, 255–260 (2013).
16. Ritchey, M. & Cooper, R. A. Deconstructing the posterior medial episodic network. *Trends Cogn. Sci.* **24**, 451–465 (2020).
17. Buckner, R. L. & DiNicola, L. M. The brain's default network: updated anatomy, physiology and evolving insights. *Nat. Rev. Neurosci.* **20**, 593–608 (2019).
18. Marek, S. & Dosenbach, N. U. F. The frontoparietal network: function, electrophysiology, and importance of individual precision mapping. *Dialogues Clin. Neurosci.* **20**, 133–140 (2018).
19. Andrews-Hanna, J. R., Smallwood, J. & Spreng, R. N. The default network and self-generated thought: component processes, dynamic control, and clinical relevance. *Ann. N. Y. Acad. Sci.* **1316**, 29–52 (2014).
20. Kucyi, A., Kam, J. W. Y., Andrews-Hanna, J. R., Christoff, K. & Whitfield-Gabrieli, S. Recent advances in the neuroscience of spontaneous and off-task thought: implications for mental health. *Nat. Ment. Health* **1**, 827–840 (2023).
21. Christoff, K., Gordon, A. M., Smallwood, J., Smith, R. & Schooler, J. W. Experience sampling during fMRI reveals default network and executive system contributions to mind wandering. *Proc. Natl. Acad. Sci. USA* **106**, 8719–8724 (2009).
22. Stawarczyk, D., Majerus, S., Maquet, P. & D'Argembeau, A. Neural correlates of ongoing conscious experience: both task-unrelatedness and stimulus-independence are related to default network activity. *PLoS ONE* **6**, e16997 (2011).
23. Fox, K. C. R., Spreng, R. N., Ellamil, M., Andrews-Hanna, J. R. & Christoff, K. The wandering brain: meta-analysis of functional neuroimaging studies of mind-wandering and related spontaneous thought processes. *NeuroImage* **111**, 611–621 (2015).
24. Kam, J. W. Y. et al. Default network and frontoparietal control network theta connectivity supports internal attention. *Nat. Hum. Behav.* **3**, 1263–1270 (2019).
25. Smallwood, J., Brown, K., Baird, B. & Schooler, J. W. Cooperation between the default mode network and the frontal–parietal network in the production of an internal train of thought. *Brain Res.* **1428**, 60–70 (2012).
26. Gonzalez-Castillo, J., Kam, J. W. Y., Hoy, C. W. & Bandettini, P. A. How to interpret resting-state fMRI: ask your participants. *J. Neurosci.* **41**, 1130–1141 (2021).
27. Gonzalez-Castillo, J. et al. In-scanner thoughts shape resting-state functional connectivity: how participants "rest" matters. Preprint at https://doi.org/10.1101/2024.06.05.596482 (2024).
28. Sripada, C. & Taxali, A. Structure in the stream of consciousness: evidence from a verbalized thought protocol and automated text analytic methods. *Conscious. Cogn.* **85**, 103007 (2020).
29. Raffaelli, Q. et al. The think aloud paradigm reveals differences in the content, dynamics and conceptual scope of resting state thought in trait brooding. *Sci. Rep.* **11**, 19362 (2021).
30. Li, H.-X. et al. Neural representations of self-generated thought during think-aloud fMRI. *NeuroImage* **265**, 119775 (2023).
31. Li, H.-X. et al. Exploring self-generated thoughts in a resting state with natural language processing. *Behav. Res. Methods* **54**, 1725–1743 (2022).
32. Raffaelli, Q. et al. Creative minds at rest: creative individuals are more associative and engaged with their idle thoughts. *Creat. Res. J.* **36**, 396–412 (2024).
33. Mallett, R., Nahas, Y., Christoff, K., Paller, K. & Mills, C. Cognitive control and semantic thought variability across sleep and wakefulness. *Phil. Mind Sci.* **6** https://doi.org/10.33735/phimisci.2025.10307 (2025)
34. Smallwood, J., Fitzgerald, A., Miles, L. K. & Phillips, L. H. Shifting moods, wandering minds: negative moods lead the mind to wander. *Emotion* **9**, 271–276 (2009).
35. Schaefer, A. et al. Local-global parcellation of the human cerebral cortex from intrinsic functional connectivity MRI. *Cereb. Cortex* **28**, 3095–3114 (2018).
36. Karapanagiotidis, T., Bernhardt, B. C., Jefferies, E. & Smallwood, J. Tracking thoughts: exploring the neural architecture of mental time travel during mind-wandering. *NeuroImage* **147**, 272–281 (2017).

37. Smallwood, J. et al. The default mode network in cognition: a topographical perspective. *Nat. Rev. Neurosci.* **22**, 503–513 (2021).
38. Yeshurun, Y., Nguyen, M. & Hasson, U. The default mode network: where the idiosyncratic self meets the shared social world. *Nat. Rev. Neurosci.* **22**, 181–192 (2021).
39. Mills, C., Herrera-Bennett, A., Faber, M. & Christoff, K. Why the mind wanders: how spontaneous thought's default variability may support episodic efficiency and semantic optimization. in *The Oxford Handbook of Spontaneous Thought: Mind-Wandering, Creativity, and Dreaming* (eds Christoff, K. & Fox, K. C. R.) 1 (Oxford University Press, 2018).
40. Duncan, K., Sadanand, A. & Davachi, L. Memory's penumbra: episodic memory decisions induce lingering mnemonic biases. *Science* **337**, 485–487 (2012).
41. Patil, A. & Duncan, K. Lingering cognitive states shape fundamental mnemonic abilities. *Psychol. Sci.* **29**, 45–55 (2018).
42. Tarder-Stoll, H., Jayakumar, M., Dimsdale-Zucker, H. R., Günseli, E. & Aly, M. Dynamic internal states shape memory retrieval. *Neuropsychologia* **138**, 107328 (2020).
43. Kim, B., Andrews-Hanna, J. R., Han, J., Lee, E. & Woo, C.-W. When self comes to a wandering mind: brain representations and dynamics of self-generated concepts in spontaneous thought. *Sci. Adv.* **8**, eabn8616 (2022).
44. Andrews-Hanna, J. R. et al. The conceptual building blocks of everyday thought: tracking the emergence and dynamics of ruminative and nonruminative thinking. *J. Exp. Psychol. Gen*. https://doi.org/10.1037/xge0001096 (2021).
45. Romney, A. K., Brewer, D. D. & Batchelder, W. H. Predicting clustering from semantic structure. *Psychol. Sci.* **4**, 28–34 (1993).
46. Abbott, J. T., Austerweil, J. L. & Griffiths, T. L. Random walks on semantic networks can resemble optimal foraging. *Psychol. Rev.* **122**, 558–569 (2015).
47. Mills, C., Zamani, A., White, R. & Christoff, K. Out of the blue: understanding abrupt and wayward transitions in thought using probability and predictive processing. *Philos. Trans. R. Soc. B Biol. Sci.* **376**, 20190692 (2021).
48. Kurby, C. A. & Zacks, J. M. Segmentation in the perception and memory of events. *Trends Cogn. Sci.* **12**, 72–79 (2008).
49. Ben-Yakov, A. & Henson, R. N. The hippocampal film editor: sensitivity and specificity to event boundaries in continuous experience. *J. Neurosci.* **38**, 10057–10068 (2018).
50. DuBrow, S. & Davachi, L. Temporal binding within and across events. *Neurobiol. Learn. Mem.* **134**, 107–114 (2016).
51. Wang, Y. C., Adcock, R. A. & Egner, T. Toward an integrative account of internal and external determinants of event segmentation. *Psychon. Bull. Rev*. https://doi.org/10.3758/s13423-023-02375-2 (2023).
52. Geerligs, L. et al. A partially nested cortical hierarchy of neural states underlies event segmentation in the human brain. *eLife* **11**, e77430 (2022).
53. Baldassano, C. et al. Discovering event structure in continuous narrative perception and memory. *Neuron* **95**, 709–721.e5 (2017).
54. Silva, M., Baldassano, C. & Fuentemilla, L. Rapid memory reactivation at movie event boundaries promotes episodic encoding. *J. Neurosci.* **39**, 8538–8548 (2019).
55. Zamani, A., Carhart-Harris, R. & Christoff, K. Prefrontal contributions to the stability and variability of thought and conscious experience. *Neuropsychopharmacology* **47**, 329–348 (2022).
56. Dixon, M. L. et al. Heterogeneity within the frontoparietal control network and its relationship to the default and dorsal attention networks. *Proc. Natl. Acad. Sci. USA* **115**, E1598–E1607 (2018).
57. Menon, V. 20 years of the default mode network: a review and synthesis. *Neuron* **111**, 2469–2487 (2023).
58. Kucyi, A. et al. Individual variability in neural representations of mind-wandering. *Netw. Neurosci*. 1–66 https://doi.org/10.1162/netn_a_00387 (2024).
59. Kérébel, A., Caille, J.-A. & Sackur, J. Dynamics of spontaneous thoughts: exploration, attentional profile and the segmentation of the stream of thoughts. *Conscious. Cogn.* **124**, 103735 (2024).
60. Tseng, J. & Poppenk, J. Brain meta-state transitions demarcate thoughts across task contexts exposing the mental noise of trait neuroticism. *Nat. Commun.* **11**, 3480 (2020).
61. Wang, Y. C. & Egner, T. Switching task sets creates event boundaries in memory. *Cognition* **221**, 104992 (2022).
62. Vandierendonck, A., Liefooghe, B. & Verbruggen, F. Task switching: interplay of reconfiguration and interference control. *Psychol. Bull.* **136**, 601–626 (2010).
63. Dosenbach, N. U. F. et al. A core system for the implementation of task sets. *Neuron* **50**, 799–812 (2006).
64. Lemire-Rodger, S. et al. Inhibit, switch, and update: a within-subject fMRI investigation of executive control. *Neuropsychologia* **132**, 107134 (2019).
65. Poldrack, R. A. Can cognitive processes be inferred from neuroimaging data?. *Trends Cogn. Sci.* **10**, 59–63 (2006).
66. Iwata, T. et al. Hippocampal sharp-wave ripples correlate with periods of naturally occurring self-generated thoughts in humans. *Nat. Commun.* **15**, 4078 (2024).
67. Ben-Yakov, A., Eshel, N. & Dudai, Y. Hippocampal immediate poststimulus activity in the encoding of consecutive naturalistic episodes. *J. Exp. Psychol. Gen.* **142**, 1255–1263 (2013).
68. Fernandino, L. & Binder, J. R. How does the "default mode" network contribute to semantic cognition?. *Brain Lang.* **252**, 105405 (2024).
69. Kam, J. W. Y. et al. Distinct electrophysiological signatures of task-unrelated and dynamic thoughts. *Proc. Natl. Acad. Sci. USA* **118**, e2011796118 (2021).
70. Beaty, R. E., Benedek, M., Silvia, P. J. & Schacter, D. L. Creative cognition and brain network dynamics. *Trends Cogn. Sci.* **20**, 87–95 (2016).
71. Ergorul, C. & Eichenbaum, H. The hippocampus and memory for "what," "where," and "when". *Learn. Mem.* **11**, 397–405 (2004).
72. Epstein, R. & Kanwisher, N. A cortical representation of the local visual environment. *Nature* **392**, 598–601 (1998).
73. Qin, P. & Northoff, G. How is our self related to midline regions and the default-mode network?. *NeuroImage* **57**, 1221–1233 (2011).
74. Buckner, R. L. & Carroll, D. C. Self-projection and the brain. *Trends Cogn. Sci.* **11**, 49–57 (2007).
75. Mulholland, B. et al. Patterns of ongoing thought in the real world. *Conscious. Cogn.* **114**, 103530 (2023).
76. Ericsson, K. A. & Simon, H. A. How to study thinking in everyday life: contrasting think-aloud protocols with descriptions and explanations of thinking. *Mind Cult. Act.* **5**, 178–186 (1998).
77. Jordano, M. L. & Touron, D. R. How often are thoughts metacognitive? Findings from research on self-regulated learning, think-aloud protocols, and mind-wandering. *Psychon. Bull. Rev.* **25**, 1269–1286 (2018).
78. Fernyhough, C. & Borghi, A. M. Inner speech as language process and cognitive tool. *Trends Cogn. Sci*. https://doi.org/10.1016/j.tics.2023.08.014 (2023).
79. Feuerriegel, S. et al. Using natural language processing to analyse text data in behavioural science. *Nat. Rev. Psychol.* **4**, 96–111 (2025).
80. Fenerci, C., Cheng, Z., Addis, D. R., Bellana, B. & Sheldon, S. Studying memory narratives with natural language processing. *Trends Cogn. Sci*. https://doi.org/10.1016/j.tics.2025.02.003 (2025).
81. Michelmann, S., Kumar, M., Norman, K. A. & Toneva, M. Large language models can segment narrative events similarly to humans. *Behav. Res. Methods* **57**, 39 (2025).

82. Li, H.-X. et al. Characterizing human spontaneous thoughts and its application in major depressive disorder. *J. Affect. Disord.* **365**, 276–284 (2024).
83. Kam, J. W. Y. et al. On the relationship between unprompted thought and affective well-being: a systematic review and meta-analysis. *Psychol. Bull.* **150**, 621–641 (2024).
84. Mulholland, B. et al. Patterns of ongoing thought in the real world and their link to mental health and well-being. Preprint at https://doi.org/10.1101/2024.07.22.604681 (2024).
85. Lee, Y. & Chen, J. The relationship between event boundary strength and pattern shifts across the cortical hierarchy during naturalistic movie-viewing. *J. Cogn. Neurosci.* **36**, 2317–2342 (2024).
86. Zacks, J. M., Speer, N. K., Vettel, J. M. & Jacoby, L. L. Event understanding and memory in healthy aging and dementia of the Alzheimer type. *Psychol. Aging* **21**, 466–482 (2006).
87. Speer, N. K., Swallow, K. M. & Zacks, J. M. Activation of human motion processing areas during event perception. *Cogn. Affect. Behav. Neurosci.* **3**, 335–345 (2003).
88. Sasmita, K. & Swallow, K. M. Measuring event segmentation: an investigation into the stability of event boundary agreement across groups. *Behav. Res. Methods* **55**, 428–447 (2023).
89. Fischl, B. FreeSurfer. *NeuroImage* **62**, 774–781 (2012).
90. Esteban, O. et al. FMRIPrep: a robust preprocessing pipeline for functional MRI. *Nat. Methods* **16**, 111–116 (2019).
91. Smith, S. M. & Brady, J. M. SUSAN—a new approach to low level image processing. *Int. J. Comput. Vis.* **23**, 45–78 (1997).
92. Yeo, T. et al. The organization of the human cerebral cortex estimated by intrinsic functional connectivity. *J. Neurophysiol.* **106**, 1125–1165 (2011).
93. Lee, H. & Chen, J. Predicting memory from the network structure of naturalistic events. *Nat. Commun.* **13**, 4235 (2022).
94. Lee, H., Li, X., Born, S., Honey, C. & Chen, J. ThinkAloud. OpenNeuro https://doi.org/10.18112/openneuro.ds006067.v1.0.0 (2025).
95. Su, H. et al. Neural dynamics of spontaneous memory recall and future thinking in the continuous flow of thoughts. *Zenodo* https://doi.org/10.5281/zenodo.15665444 (2025).
96. Lee, H., Chen, J. & Hasson, U. FilmFestival. OpenNeuro https://doi.org/10.18112/openneuro.ds004042.v1.0.1 (2022).
97. Lee, H., Chen, J. & Hasson, U. A functional neuroimaging dataset acquired during naturalistic movie watching and narrated recall of a series of short cinematic films. *Data Brief.* **46**, 108788 (2023).

Acknowledgements

We thank Yoonjung Lee for assisting with collecting fMRI data and Colette Youstra for assisting with collecting behavioral thought segmentation data. C.J.H. was supported by National Institute of Mental Health (R01MH119099) and National Science Foundation CAREER Award (BCS-2238711). J.C. was supported by National Institute of Mental Health (R01MH133732).

Author contributions

H.L. conceived and designed the research. X.L., S.B., J.C. and H.L. collected the data. H.L. analyzed the data. H.S. and H.L. wrote the original manuscript. H.S., C.J.H., J.C. and H.L. reviewed and edited the manuscript. C.J.H., J.C. and H.L. provided funding.

Competing interests

The authors declare no competing interests.

Additional information

Supplementary information The online version contains supplementary material available at https://doi.org/10.1038/s41467-025-61807-w.

Correspondence and requests for materials should be addressed to Hongmi Lee.

Peer review information *Nature Communications* thanks Aaron Kucyi and the other, anonymous, reviewer(s) for their contribution to the peer review of this work. A peer review file is available.